General Disclaimer

One or more of the Following Statements may affect this Document

- This document has been reproduced from the best copy furnished by the organizational source. It is being released in the interest of making available as much information as possible.

- This document may contain data, which exceeds the sheet parameters. It was furnished in this condition by the organizational source and is the best copy available.

- This document may contain tone-on-tone or color graphs, charts and/or pictures, which have been reproduced in black and white.

- This document is paginated as submitted by the original source.

- Portions of this document are not fully legible due to the historical nature of some of the material. However, it is the best reproduction available from the original submission.

NAS CR-134626
TRW ER-7723

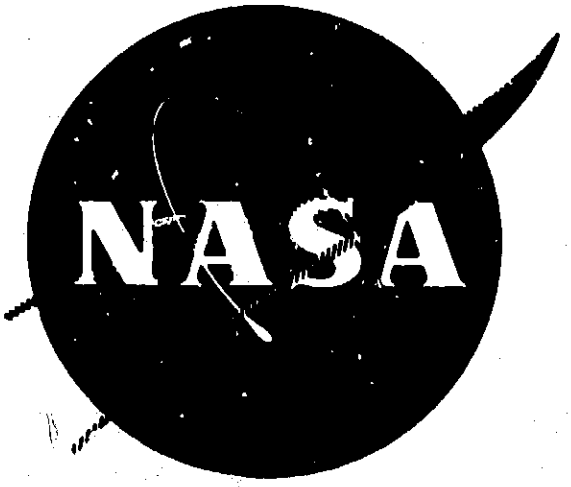

THE PARTITIONED STRAINRANGE FATIGUE BEHAVIOR OF COATED AND UNCOATED MAR-M-302 AT 1000°C (1832°F) IN ULTRAHIGH VACUUM

by
K.D. SHEFFLER

FINAL REPORT

Prepared for

NATIONAL AERONAUTICS AND SPACE ADMINISTRATION

UNDER CONTRACT NAS-3-17786
G. R. HALFORD, Project Manager

TRW MATERIALS TECHNOLOGY LABORATORIES
CLEVELAND, OHIO

FOREWORD

The work described in this report was performed in the Materials Technology Laboratory of TRW Inc. under sponsorship of the National Aeronautics and Space Administration, Contract NAS-3-17786. The program was administered for TRW by Mr. J. A. Alexander, Program Manager. The Principal Investigator was Dr. K. D. Sheffler, with technical assistance provided by Mr. J. W. Sweeney. The NASA Technical Manager was Dr. G. R. Halford.

Prepared by: K. D. Sheffler
K. D. Sheffler
Principal Engineer

Approved by: John A. Alexander
J. A. Alexander
Manager
Materials Research Department

FOREWORD

The work described in this report was performed in the Materials Technology Laboratory of TRW Inc. under sponsorship of the National Aeronautics and Space Administration, Contract NAS-3-17786. The program was administered for TRW by Mr. J. A. Alexander, Program Manager. The Principal Investigator was Dr. K. D. Sheffler, with technical assistance provided by Mr. J. W. Sweeney. The NASA Technical Manager was Dr. G. R. Halford.

Prepared by: K. D. Sheffler

K. D. Sheffler
Principal Engineer

Approved by: John A. Alexander

J. A. Alexander
Manager
Materials Research Department

SUMMARY

A primary purpose of this program was to investigate the influence of environment and an aluminide coating (PWA 45) on the partitioned strainrange fatigue behavior of a cobalt-base MAR-M-302 alloy. To accomplish this, comparative fatigue tests were conducted on coated and uncoated samples with the four basic types of thermal-mechanical strain cycles (wave shapes) defined by the method of strainragne partitioning. All tests were conducted in an ultra-high vacuum to eliminate the confounding effects of environmental interactions on elevated temperature behavior. Maximum test temperature was 1000°C (1832°F).

Results of these tests indicated no significant influence of the aluminide coating on MAR-M-302 fatigue life for ε_{pp}, ε_{cc} and ε_{cp} types of cycling. Indirect evidence indicated that this conclusion could be extended to the ε_{pc} type of cycle as well.

The test results showed a significant dependence of fatigue life on the type of thermal-mechanical cycle (wave shape) applied. Fatigue life was greatest with the ε_{pp} cycle, and was reduced by about 1/2 to 1 order of magnitude by ε_{cc} cycling. Application of the ε_{cp} cycle caused a life reduction of between 1-1/2 and 2 orders of magnitude while the ε_{pc} life appeared to be comparable to the ε_{cc} life. The occurrence of fatigue life variations with these different types of thermal-mechanical fatigue cycles in the absence of environmental interactions served to emphasize the importance of creep-fatigue interactions in elevated temperature fatigue behavior. The concept of strainrange partitioning appears to offer an appropriate framework around which this behavior can be characterized.

TABLE OF CONTENTS

1 INTRODUCTION

Aluminide coatings are widely used in airbreathing turbine engines for improvement of oxidation and hot corrosion resistance of critical hot section components. While satisfactory for this purpose, such coatings may degrade the mechanical properties of coated hardware. Of particular concern is a reduction of fatigue resistance in complex geometry hot section structures such as turbine blades and vanes which experience severe thermal-mechanical strain cycling during engine service.

To study this problem a program was undertaken to simulate the thermal-mechanical fatigue behavior of a cobalt-base superalloy (MAR-M-302) in the coated (PWA 45) and uncoated condition. This program involved closed-loop, servo-controlled fatigue testing with synchronized, independently programmed temperature and strain cycling to develop baseline data for analysis of thermal fatigue behavior by the method of strainrange partioning (1). Tests were performed in air and in vacuum to separate the effects of environmental interactions from mechanical effects of the coating on fatigue behavior. The program was a cooperative effort between the Materials Technology Laboratory of TRW Inc. and the Materials and Structures Division of the NASA Lewis Research Center, with vacuum tests being performed at TRW and air testing at NASA. This report presents the results of the vacuum fatigue tests performed at TRW.

Experimental Details

Equipment and procedures used for vacuum thermal fatigue tests on this program have been described in detail in previous reports (2,3). Briefly, tests were conducted on coated and uncoated tubular hourglass specimens provided by the sponsor (Figure 1) with closed-loop diametral strain control in an ultrahigh vacuum chamber at pressures below 1×10^{-7} torr. Synchronized thermal cycling was accomplished by direct resistance heating using a programmable thyratron controlled 50 KVA power source. The measured specimen diameter was compensated electronically for thermal expansion so that net mechanical strain was controlled directly. Load, diameter and temperature were recorded continuously, with load-diameter hysteresis loops being obtained at periodic intervals during each test. Failure was defined as separation of the specimen into two pieces.

While no major difficulties were encountered in changing from the original solid hourglass specimen design (2) to the tubular specimen, one minor problem was encountered which involved a tendency for the servo-control system to become unstable at fracture. This instability resulted in the application of large, uncontrolled compressive strains at failure, which rewelded the specimen and caused the hollow tube to essentially collapse under the relatively light spring pressure of the diametral extensometer (Figure 2). While causing no major problem in generation of the required test data, this behavior was annoying because it eliminated the possibility for meaningful interpretation of microstructural damage in a number of the tested specimens.

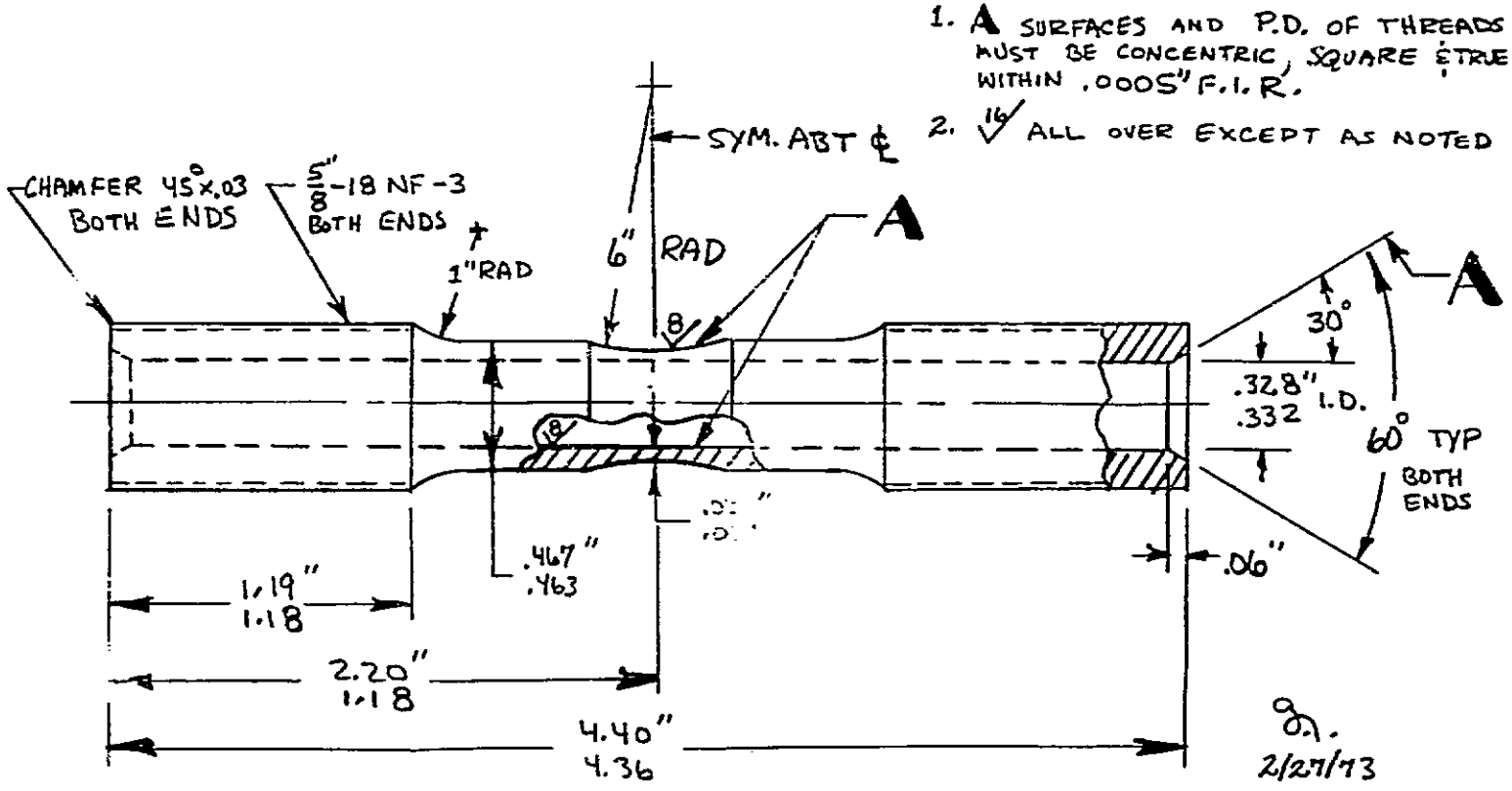

Figure 1. Thermal-Mechanical Fatigue Test Specimen.

Figure 2. Photograph of Specimen Which Underwent Uncontrolled Compressive Loading at Failure as a Result of Dynamic Control Instability Accompanying Fracture.

The test program involved both isothermal and thermal-mechanical strain cycling to measure the four basic types of creep-fatigue life relationships defined by the strainrange partitioning analysis (Reference 1). The ε_{pp} and ε_{cc} curves were obtained from 1000°C (1832°F) isothermal tests conducted at 0.65 and 0.0065 Hz, respectively, while ε_{cp} and ε_{pc} curves were determined using a test cycle where temperature and strain were varied sequentially so that both tensile and compressive deformation occurred isothermally but at different temperatures (Figure 3). In all cases, the diametral strain was varied linearly with time. The TCIPS* cycle was used to determine fatigue life for ε_{cp} type deformation, while ε_{pc} behavior was evaluated using the TCOPS** type of cycle (1,3). Specific conditions of temperature and frequency are indicated in Table 1 for each test together with the inelastic and total longitudinal strainranges applied. In addition to these basic cycle types, a special series of tests were performed to determine the percentage of time-dependent (creep) deformation associated with each of the inelastic strain ranges investigated. The purpose of these tests was to confirm that the majority of the reversed inelastic strain imposed at 1000°C (1832°F) and 0.0065 Hz was indeed thermally activated as assumed in the use of this temperature and frequency for definition of the ε_{cc}, ε_{cp} and ε_{pc} lines. Details of the procedures and results from these tests are given in Appendix A.

Because the data presented in this report represent one-half of a test program to be completed on different test equipment, it was considered desirable to conduct supplementary tests in air on the TRW equipment for direct comparison with tests conducted on the NASA system used for generation of the air data. Because of a shortage of MAR-M-302 test material, isothermal tests were conducted on 316 stainless steel specimens at a temperature and frequency of 705°C (1300°F) and 0.0167 Hz for comparison with previous data generated on the Lewis test equipment.

* Thermal Cycle In-Phase with Strain
** Thermal Cycle Out-of-Phase with Strain

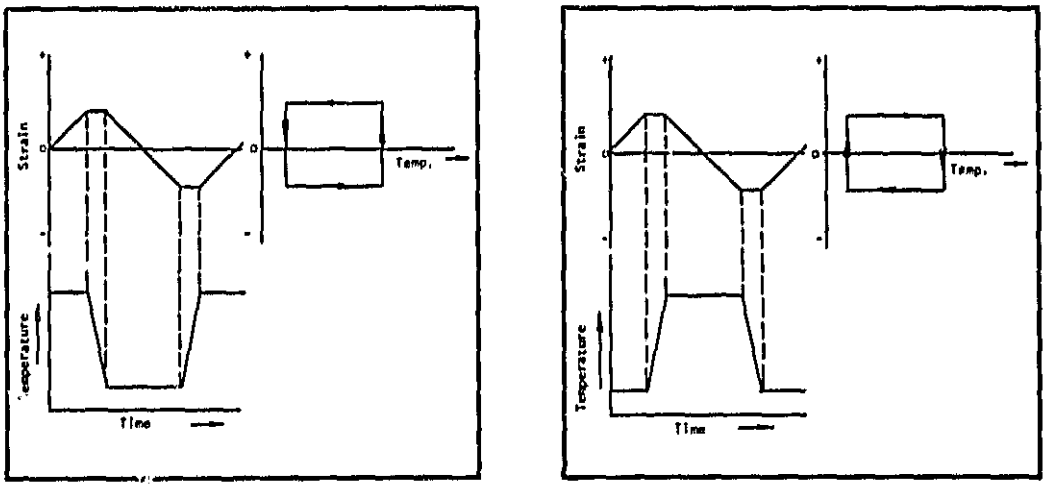

(a) TCIPS

Used to measure ε_{cp} curve

(b) TCOPS

Used to measure ε_{pc} curve

Figure 3. Schematic Representation of the Two Types of Thermal-Mechanical Cycles Applied in this Study.

II RESULTS AND DISCUSSION

1. Cyclic Stress-Strain Behavior

Dynamic stress-strain response (hysteresis loops) and stress versus cycle curves are presented in Appendices B and C. The stress-cycle indicated a general trend for cyclic strain hardening, although the data were not entirely consistent from test to test. For example, for uncoated material cycled isothermally at 1000°C (1832°F) and 0.0065 Hz, the specimen tested at 0.00671 total longitudinal strain range (Figure C-2) exhibited a definite hardening behavior, while tests at strain ranges of 0.00301 and 0.01388 did not (Figures C-1 and C-3). This inconsistency in hardening behavior did not appear to correlate uniquely with any of the applied test parameters (strain, frequency or thermal cycle type) and was reflected in pronounced variability of the saturation stresses noted in Table 1. Because of this variability in hardening behavior, it was not possible in some cases to measure specimen life in terms of 5 and 50% load drop, as specified in the Work Statement, so that life is noted only in terms of cycles to complete separation of the specimen (Table 1). The load drops refer to the situation wherein the plots of stress versus number of cycles will show a decrease after reaching stabilization or linearity earlier in the test. This behavior also precluded presentation of hysteresis loops at 1/2 of the life to 5% load drop, as required in the Work Statement, so that instead hysteresis loops have been presented which represent the cyclic stress-strain behavior during what was judged to represent the stabilized portion of each test.

2. Influence of Cycle Parameters on Fatigue Life

Fatigue life of the coated and uncoated MAR-M-302 is plotted as a function of inelastic and total longitudinal strain range in Figure 4 for the TCIPS and the two isothermal cycle types (ε_{cp}, ε_{cc} and ε_{pp} deformation). Only test No. 55 was plotted from TCOPS results (ε_{pc} deformation), as the remaining three specimens tested with this cycle broke outside the gage section.

Two significant conclusions may be drawn from examination of these data. First, in the absence of environmental interactions, there is little, if any, influence of the aluminide coating on fatigue life of the MAR-M-302 alloy for ε_{cc}, ε_{pp} and ε_{cp} types of cycling. While a direct comparison was not possible for the ε_{pc} cycle because of failure outside the gage section, comparison of results from tests 57 and 72 (Table 1), which were conducted at comparable (although not identical) strain ranges, and failed at the same location, indicated that this conclusion extended to the ε_{pc} type cycle as well.

Table 1

Summary of MAR-M-302 Fatigue Test Results

Specimen No.	Surface Condition	Cycle Type**	Frequency Hz	Temperature Upper °F	Temperature Upper °C	Temperature Lower °F	Temperature Lower °C	Stress ksi Tensile	Stress ksi Comp.	Stress ksi Range	Stress MN/m² Tensile	Stress MN/m² Comp.	Stress MN/m² Range	Longitudinal Strain Range in/in Inelastic	Longitudinal Strain Range in/in Total	Cycles to Failure	Hours Time at T_{max}
58	Uncoated	Isothermal	0.65	1832	1000	-	-	-	-	34	-	-	234	.00059	.00301	9433	4.0+
5	Uncoated	Isothermal	0.65	1832	1000	-	-	-	-	56	-	-	385	.00438	.00671	968	0.4+
16	Uncoated	Isothermal	0.65	1832	1000	-	-	-	-	69	-	-	475	.01100	.01388	245	0.1+
1	Coated	Isothermal	0.65	1832	1000	-	-	-	-	52	-	-	358	.00313	.00530	2239	1.0+
2	Coated	Isothermal	0.65	1832	1000	-	-	-	-	71.5	-	-	492	.00862	.01160	201	0.1+
23	Uncoated	Isothermal	0.0065	1832	1000	-	-	-	-	32	-	-	220	.00291	.00424	364	15.6+
61	Uncoated	Isothermal	0.0065	1832	1000	-	-	-	-	22	-	-	151	.00789	.00881	90	3.9+
7	Uncoated	Isothermal	0.0065	1832	1000	-	-	-	-	35	-	-	241	.00944	.01090	52	2.2+
17	Coated	Isothermal	0.0065	1832	1000	-	-	-	-	35	-	-	241	.00281	.00427	511	10.9+
12	Coated	Isothermal	0.0065	1832	1000	-	-	-	-	46	-	-	316	.00813	.01005	95	2.0+
49	Uncoated	TCIPS	0.0065	1832	1000	932	500	17	63.5	80.5	117	437	554	.00132	.00408	71	1.5+
33	Uncoated	TCIPS	0.0065	1832	1000	932	500	19	70	89	131	482	613	.00590	.00895	14	0.3+
59	Coated	TCIPS	0.0065	1832	1000	932	500	19	82.5	101.5	131	568	699	.00095	.00444	72	1.5+
26	Coated	TCIPS	0.0065	1832	1000	932	500	20.5	73.5	94	141	506	647	.00539	.00861	16	0.6+
55	Uncoated	TCOPS	0.0065	1832	1000	932	500	60	10	70	413	69	482	.00169	.00405	1308	28.0+
57	Uncoated	TCOPS	0.0065	1832	1000	932	500	97	19	116	667	131	798	.00734	.01126	64*	1.4+
76	Coated	TCOPS	0.0065	1832	1000	932	500	65	12	77	447	83	530	.00150	.00410	515*	11.0+
72	Coated	TCOPS	0.0065	1832	1000	932	500	82	13	95	564	90	654	.00620	.00939	75*	1.6+

* Specimen failed outside gage section.

** TCIPS - Thermal cycled in phase square wave (tension isothermal hot, compression isothermal cold).
TCOPS - Thermal cycled out-of-phase square wave (tension isothermal cold, compression isothermal hot).

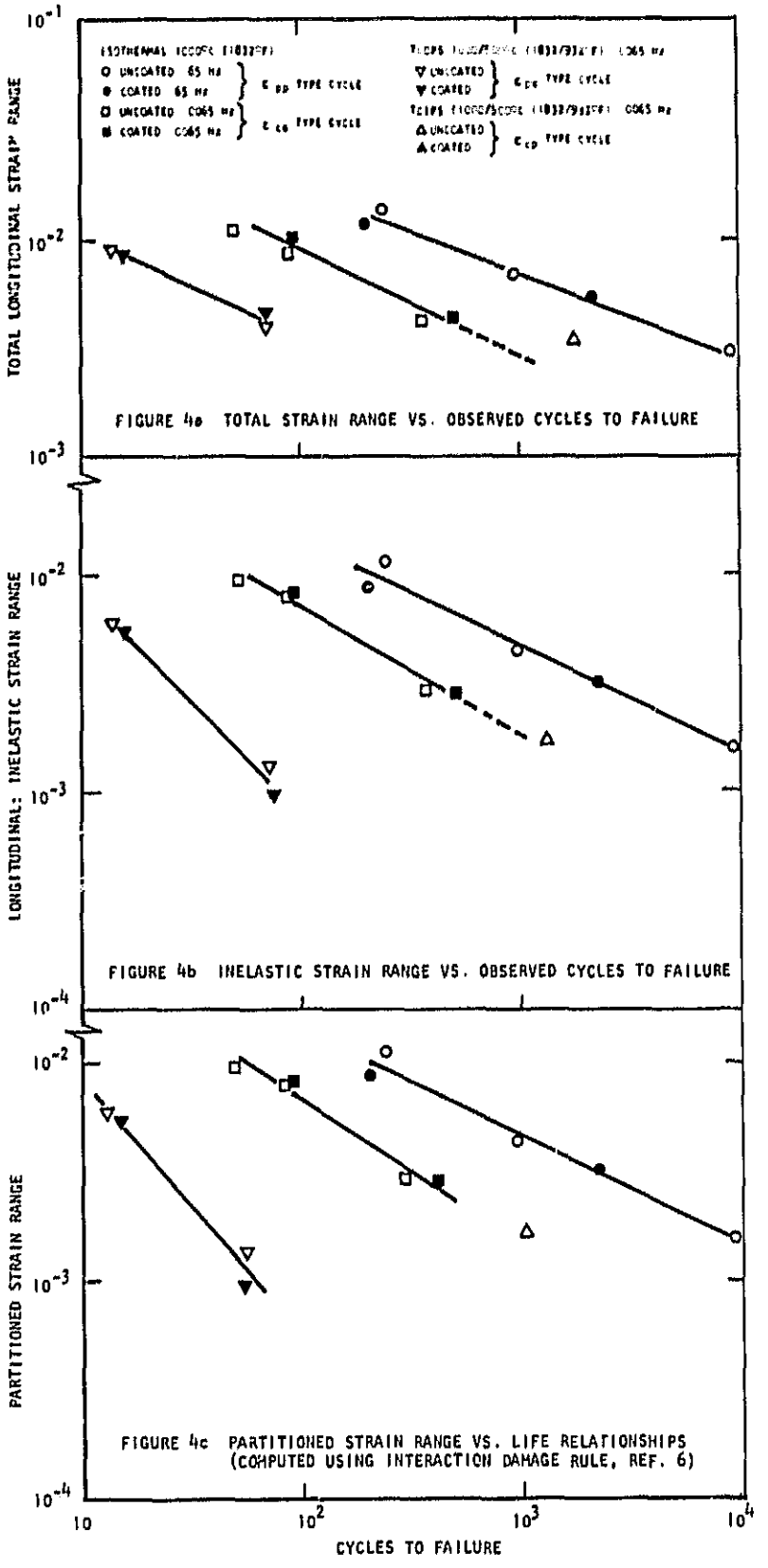

FIGURE 4a TOTAL STRAIN RANGE VS. OBSERVED CYCLES TO FAILURE

FIGURE 4b INELASTIC STRAIN RANGE VS. OBSERVED CYCLES TO FAILURE

FIGURE 4c PARTITIONED STRAIN RANGE VS. LIFE RELATIONSHIPS (COMPUTED USING INTERACTION DAMAGE RULE, REF. 6)

Figure 4. MAR-M302 Fatigue Test Results.

The second major conclusion to be drawn from the data presented in Figure 4 is that there is a significant influence of both frequency and combined thermal-mechanical cycling (wave shape) on the fatigue life of the MAR-M-302 alloy. The role of the cycle parameters, frequency and wave shape, is to influence the amount of creep strain and its location (tension or compression) within the cycle. A low frequency of 0.0065 Hz for the isothermal continuous strain cycle produces a hysteresis loop with a significant amount of creep strain in both the tensile and compressive halves of the cycle (ε_{cc}). The effect of the in-phase thermal-mechanical strain cycle is to introduce significant creep into only the tensile half of the hysteresis loop (ε_{cp}). Similarly, the out-of-phase thermal-mechanical strain cycle produces creep strain in only the compressive half of the hysteresis loop (ε_{pc}). The isothermal data show a separation of about 1/2 order of magnitude between the ε_{cc} and ε_{pp} lines when correlated on the basis of either total or inelastic strainrange, indicating significant influence of reversed creep deformation on fatigue life. The data show an even further life reduction below ε_{pp}, ranging between 1-1/2 and 2 orders of magnitude, depending on whether the inelastic or total strainrange correlation is examined, for the case of tensile creep deformation reversed by compressive plastic deformation* (ε_{cp} cycling). While a definitive conclusion regarding the effect of ε_{pc} cycling was not possible because of the fracture location on the TCOPS specimens, a comparison of the single valid ε_{pc} data point with the remaining data indicated that the fatigue life with ε_{pc} cycling was comparable to or slightly greater than isothermal life at the same frequency and at the peak temperature of the thermal cycle. (Again depending on whether the comparison is made on the basis of inelastic or total strainrange.)

3. Observations on Fracture Behavior

Figure 5 shows the typical fracture location for the ε_{pc} cycle, which was outside the hourglass area and near the end of the straight-sided portion of the reduced section. Fracture occurred at this site because of a disproportionately greater reduction of cross sectional area in this region of the specimen with respect to the original minimum diameter. This behavior has been observed previously with ε_{pc} cycling of solid hourglass tantalum and 304 stainless steel specimens in this laboratory (2,3) and on copper by Conway et al (4). No explanation is presently available for this phenomenon which limits the ability to measure intrinsic fatigue resistance with ε_{pc} cycling in materials where it occurs.

- - - - - - - - - - - - - - - -

* Following the convention established by Manson (1), the term inelastic is used in this report for any deformation which is not elastic, while the term plastic has been reserved for inelastic deformation which does not occur by time-dependant deformation mechanisms. The term creep is used in a very broad sense to indicate time-dependent deformation.

Examination of tested specimens revealed gross physical coating damage where tensile loading was applied at low temperature (ε_{pc} cycle). This damage was characterized by fine coating cracks oriented perpendicular to the tensile axis and was greatest in the area where the specimen failed (Figure 5). Similar, although less severe damage was observed on the high strainrange ε_{cc} specimen (No. 12) in the hourglass section where this specimen failed (Figure 6). This type of damage apparently had little influence on fatigue life, as evidenced by the good correlation of the results from Specimen 12 with other ε_{cc} cycle data (Figure 4).

Except for the crazing noted above, the coating appeared to behave in a ductile fashion (to be expected where loading is applied at 1000°C (1832°F)), as evidenced by the ability of the coating to conform to the surface upheaval developed by reversed plastic deformation of the substrate (Figure 7). This upheaval of the coating was apparent even in the case where severe crazing was also observed (Figure 5) and was attributed to cooperative compressive inelastic deformation of the coating-substrate system during high temperature deformation.

4. Results of Tests on 316 Stainless Steel

Results of two tests conducted on 316 stainless steel are presented in Table II and are compared with previous results generated at NASA in Figure 8. These data indicate that, within the range of reasonable experimental scatter, results from the two test systems are comparable.

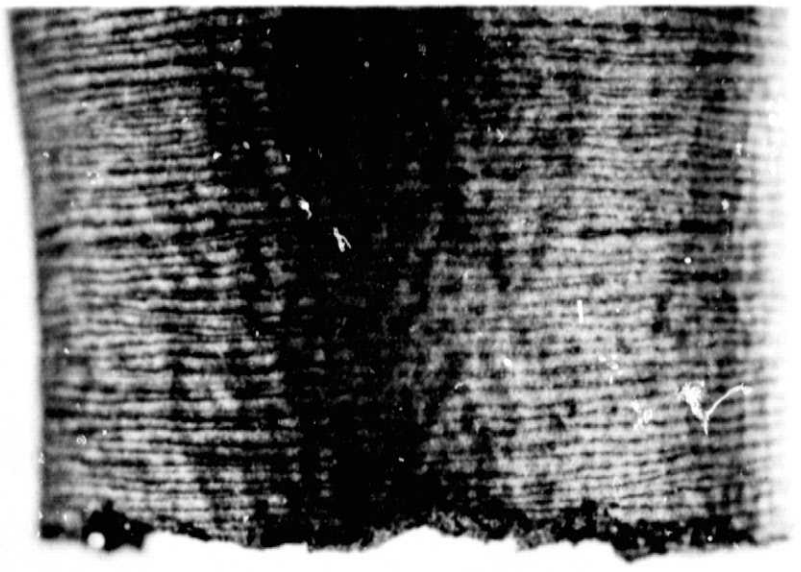

Figure 5. Coating Damage in Specimen No. 72 Tested with TCOPS (ε_{pc}) Cycling at 0.0065 Hz, 1000/500°C (1832/932°F), Total Longitudinal Strainrange .00671.

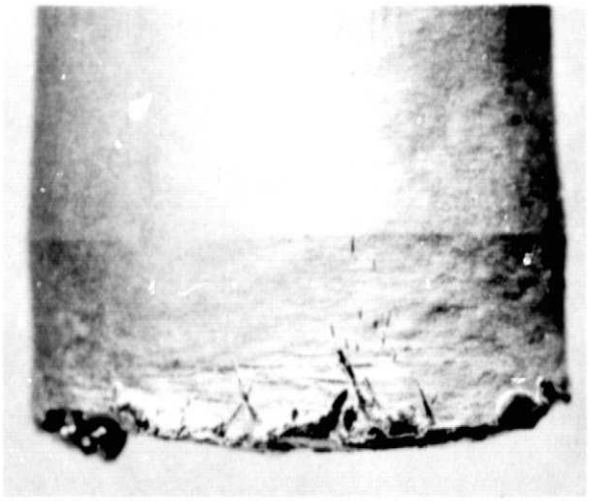

Figure 6. Coating Damage in Specimen No. 12 Tested Isothermally at 1000°C (1832°F), .0065 Hz (ε_{cc} Cycle), Total Longitudinal Strain Range .01005.

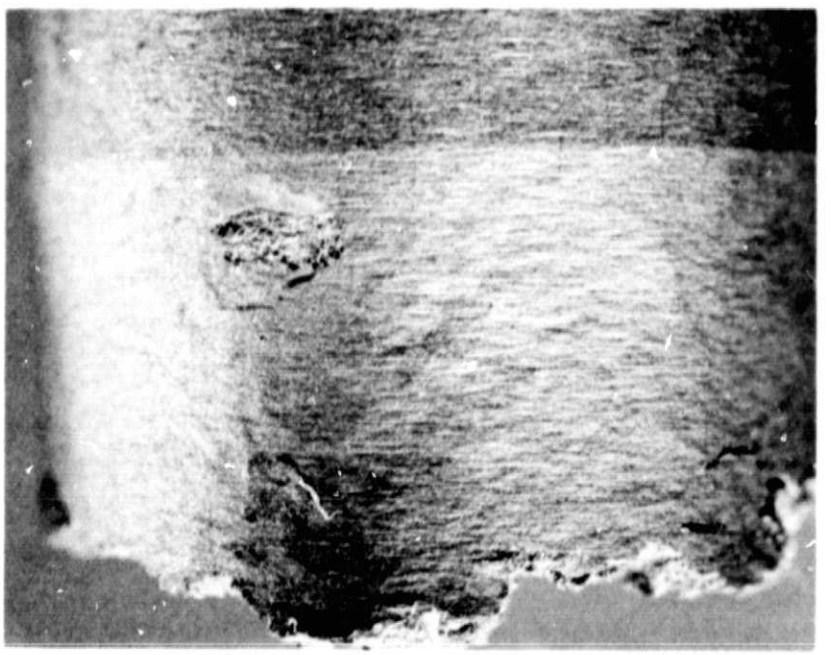

Figure 7. Surface Upheaval in Coated Specimen No. 59 Tested with TCIPS (ε_{cp}) Cycling at 0.0065 Hz, 1000/500°C (1832/932°F), Total Longitudinal Strainrange .00444.

Table II

Summary of Low Cycle Fatigue Test Results for 316 Stainless Steel Tested in Air at 705°C (1300°F), .0167 Hz (10 cpm)

Test No.	Longitudinal Strain Range		Stress Range		Cycles to Failure
	Inelastic	Total	psi	MN/m^2	
AYY 255	.01470	.02018	115.0	792	298
AYY 256	.00283	.00650	76.3	507	2297

Table II

Summary of Low Cycle Fatigue Test Results for 316 Stainless Steel Tested in Air at 705°C (1300°F), .0167 Hz (10 cpm)

Test No.	Longitudinal Strain Range		Stress Range		Cycles to Failure
	Inelastic	Total	psi	MN/m^2	
AYY 255	.01470	.02018	115.0	792	298
AYY 256	.00283	.00650	76.3	507	2297

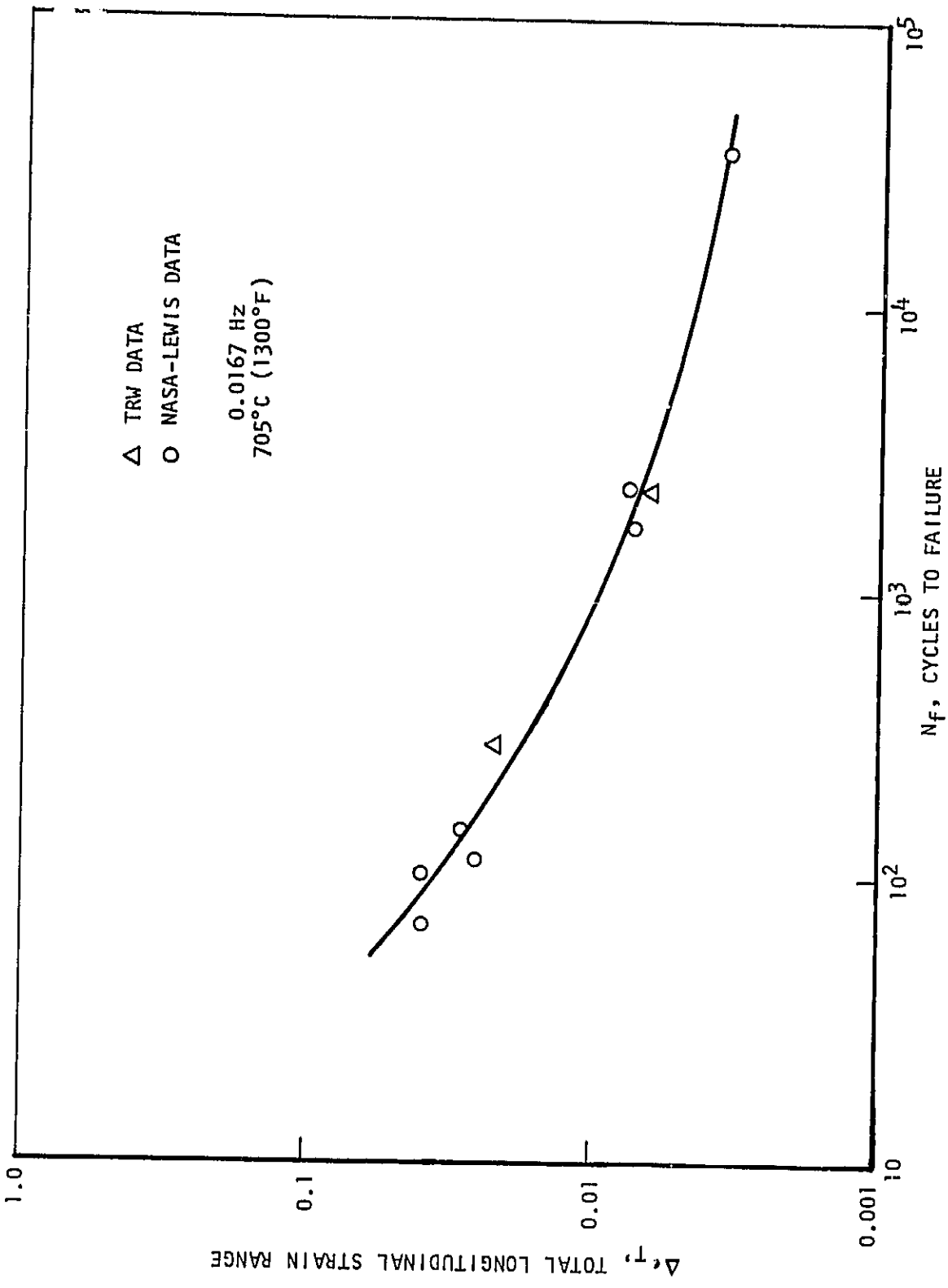

Figure 8. Comparison of 316 Stainless Steel Fatigue Data Generated on TRW and NASA Test Equipment.

III CONCLUSIONS

Results of vacuum fatigue tests conducted on uncoated and PWA 45 coated MAR-M-302 cobalt-base alloy indicated that in the absence of environmental effects there is no significant influence of the aluminide coating on the elevated temperature fatigue life of this alloy for ε_{cc}, ε_{pp} and ε_{cp} types of reversed inelastic strain cycling. Indirect evidence indicated that this conclusion could be extended to the case of ε_{pc} type of cycling as well. Examination of tested specimens indicated that fatigue life in vacuum was not influenced by the development of coating cracks oriented perpendicular to the tensile axis.

The results also indicated significant differences in the fatigue life of this alloy with each of these four types of thermal-mechanical cycles. Life was greatest with the ε_{pp} type cycle, and was reduced by about 1/2 to 1 order of magnitude by ε_{cc} type cycling. ε_{cp} type cycling caused further life reductions ranging from 1-1/2 to 2 orders of magnitude below the ε_{pp} lives, while it appeared that ε_{pc} type cycling procided about the same life as the ε_{cc} type of cycle.

The concept of strainrange partitioning appears to offer an appropriate framework around which to characterize the effects of creep on high-temperature, low-cycle fatigue.

IV REFERENCES

1. S. S. Manson, G. R. Halford and H. M. Hirschberg, "Creep-Fatigue Analysis by Strainrange Partitioning," Design for Elevated Temperature Environment, American Society of Mechanical Engineers, 1971, pp. 12-24, Discussion pp. 25-28.

2. K. D. Sheffler and G. S. Doble, "Influence of Creep Damage on the Low Cycle Thermal-Mechanical Fatigue Behavior of Two Tantalum Base Alloys," Final Report, Contract NAS-3-13228, NASA CR-121001, TRW-ER-7592, 1 May 1972.

3. K. D. Sheffler, "Vacuum Thermal-Mechanical Fatigue Testing of Two Iron Base High Temperature Alloys," Topical Report No. 3, Contract NAS-3-6010, NAS-CR-13424, TRW-ER-7696, 31 January 1974.

4. J. B. Conway, R. H. Stentz and J. T. Berling, "High Temperature, Low Cycle Fatigue of Copper-Base Alloys in Argon; Part II - Zirconium Copper at 482, 538, 593°C," NASA CR-121260, 1973.

5. S. S. Manson, "The Challenge to Unify Treatment of High Temperature Fatigue - A Partisan Proposal Based on Strainrange Partitioning," Fatigue at Elevated Temperatures, ASTM STP 520, American Society for Testing and Materials, 1973, pp. 744-782.

6. S. S. Manson and G. R. Halford, "Some New Relations and Procedures for Applying Strainrange Partitioning to High Temperature Metal Fatigue, proposed NASA Technical Note.

APPENDIX A

STRAINRANGE PARTITIONING TESTS

The purpose of this appendix is to describe procedures and results for a supplementary series of tests conducted to define the percentage of reversed inelastic strain occurring by creep, i.e., time-dependent, thermally-activated deformation mechanisms, at 1000°C (1832°F) and 0.0065 Hz. These procedures were employed at the suggestion of the Project Manager and follow the concept first described in Reference 5. Additional details are to appear in a forthcoming NASA Technical Note by S. S. Manson and G. R. Halford (Reference 6). To determine the percentage of creep strain, tests were conducted in load control with incremental cycling so that the time-at-load for each part of the cycle approximated the integrated load-time history in the same part of the continuous strain-controlled cycle to be partitioned. This technique is illustrated in Figure A-1 which shows an incremental load-time command cycle superimposed on a load-time (strain) cycle developed in continuous strain cycling. The load levels to be applied in the incremental loop were obtained from the continuous loop by arbitrarily dividing the continuous loop into eight time divisions and noting the average load achieved in the continuous loop during each time increment. The partitioning test was then conducted by manually stepping the system through the load-time loop so developed. The division of the loop into eight increments represented a compromise between approximation of the continuous load-time curve and the ability to accurately control the level and duration of the load steps in manual cycling.

Four tests were conducted using two coated and two uncoated specimens to partition the inelastic strain range at each of the two total longitudinal strain ranges indicated in Table A-1. Each specimen was precycled in strain control prior to incremental cycling to stabilize the load range and to obtain baseline hysteresis loops for determination of the load increments.

A typical load-strain output from one of the incremental loading loops is illustrated in Figure A-2. In practice, the load was reduced momentarily at the termination of each load increment to allow control adjustment as necessary to achieve the next higher load level desired. In every case this load decrement was large enough to establish a rest load below the level for significant thermally-activated deformation. Loading increments were made rapidly to minimize the amount of time dependent deformation which could occur during loading. The time-dependent strain which occurred at each constant load level was interpreted as thermally activated (creep) deformation, and the summation of the isostatic strain increments around the loop were divided by the total observed strain range to determine the percentage of the total inelastic strain cycle which occurred by creep deformation mechanisms.

Results of each of the four partitioning tests conducted in this program are summarized in Table A-1. These data indicate that more than 75% of the reversed cyclic deformation observed in the coated and uncoated MAR-M-302 alloy at 1000°C (1832°F) and 0.0065 Hz occurred by time dependent (thermally activated) deformation mechanisms, thereby supporting the choice of these test conditions for definition of the ε_{cc}, ε_{cp} and ε_{pc} fatigue life curve.

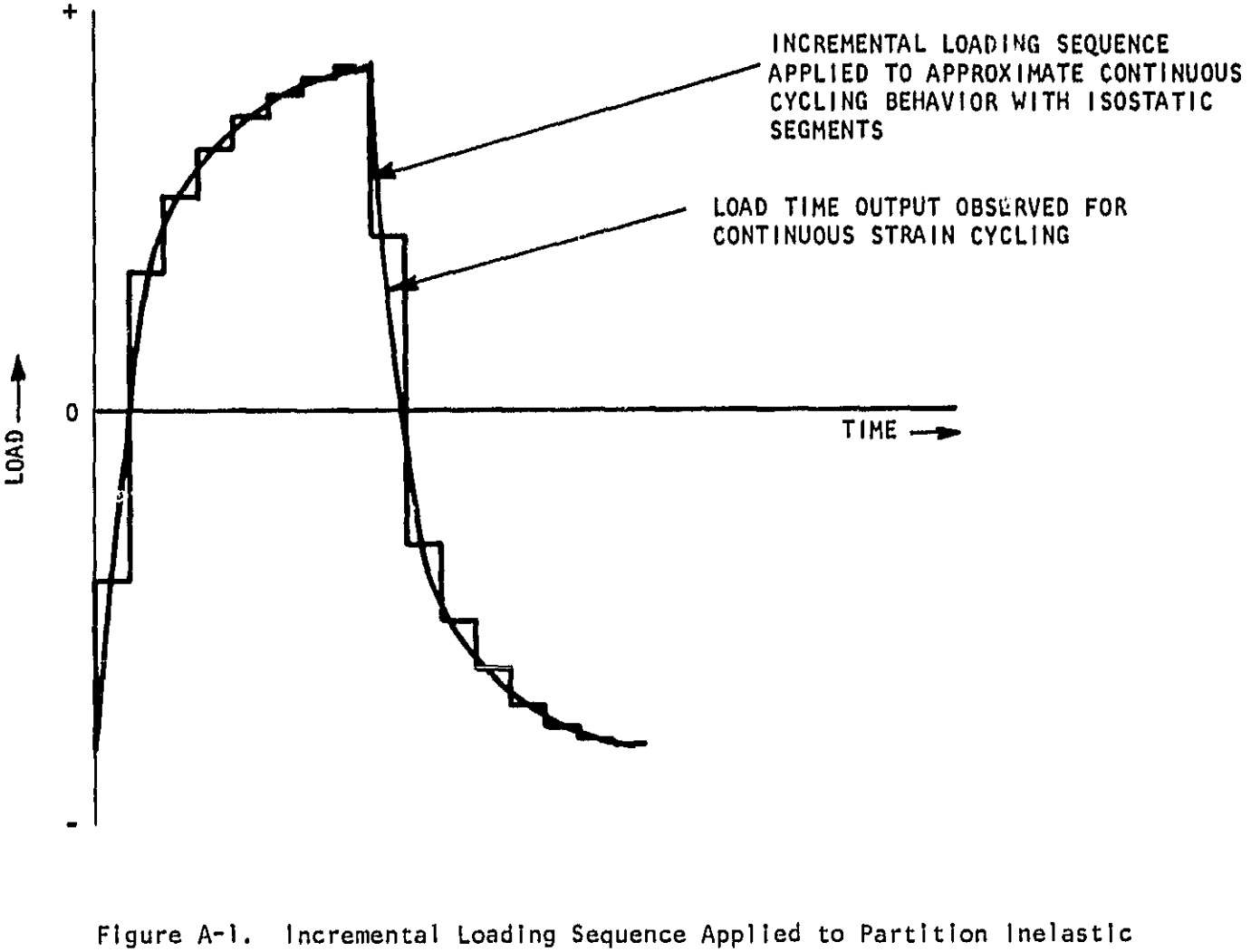

Figure A-1. Incremental Loading Sequence Applied to Partition Inelastic Strain Range.

Table A-1

Results of Strainrange Partitioning Tests

Specimen No.	Coating	Continuous Cycling Conditions					Percent of Total Inelastic Strainrange Occurring by the Dependent (creep) Deformation
		Temperature		Frequency	Longitudinal Strain Range		
		°F	°C	Hz	Inelastic	Total	
	Uncoated	1832	1000	0.0065	.00230	.00361	78
62	Uncoated	1832	1000	0.0065	.00778	.00989	92
87	Coated	1832	1000	0.0065	.00242	.00405	75
77	Coated	1832	1000	0.0065	.00720	.00935	93

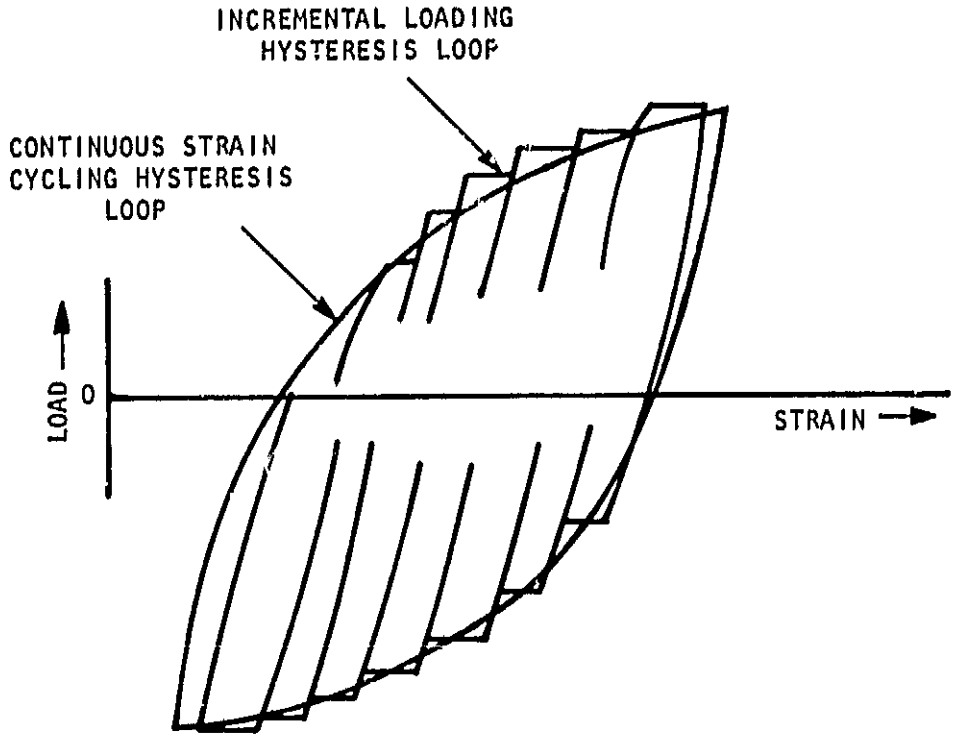

Figure A-2. Schematic Comparison of Continuous and Incremental Load-Strain Hysteresis Loops for Specimen No. 87 (Coated). Continuous Cycling Conditions 1000°C (1832°F), 0.0065 Hz, Total Longitudinal Strainrange 0.004 in/in.

APPENDIX B

HYSTERESIS LOOPS

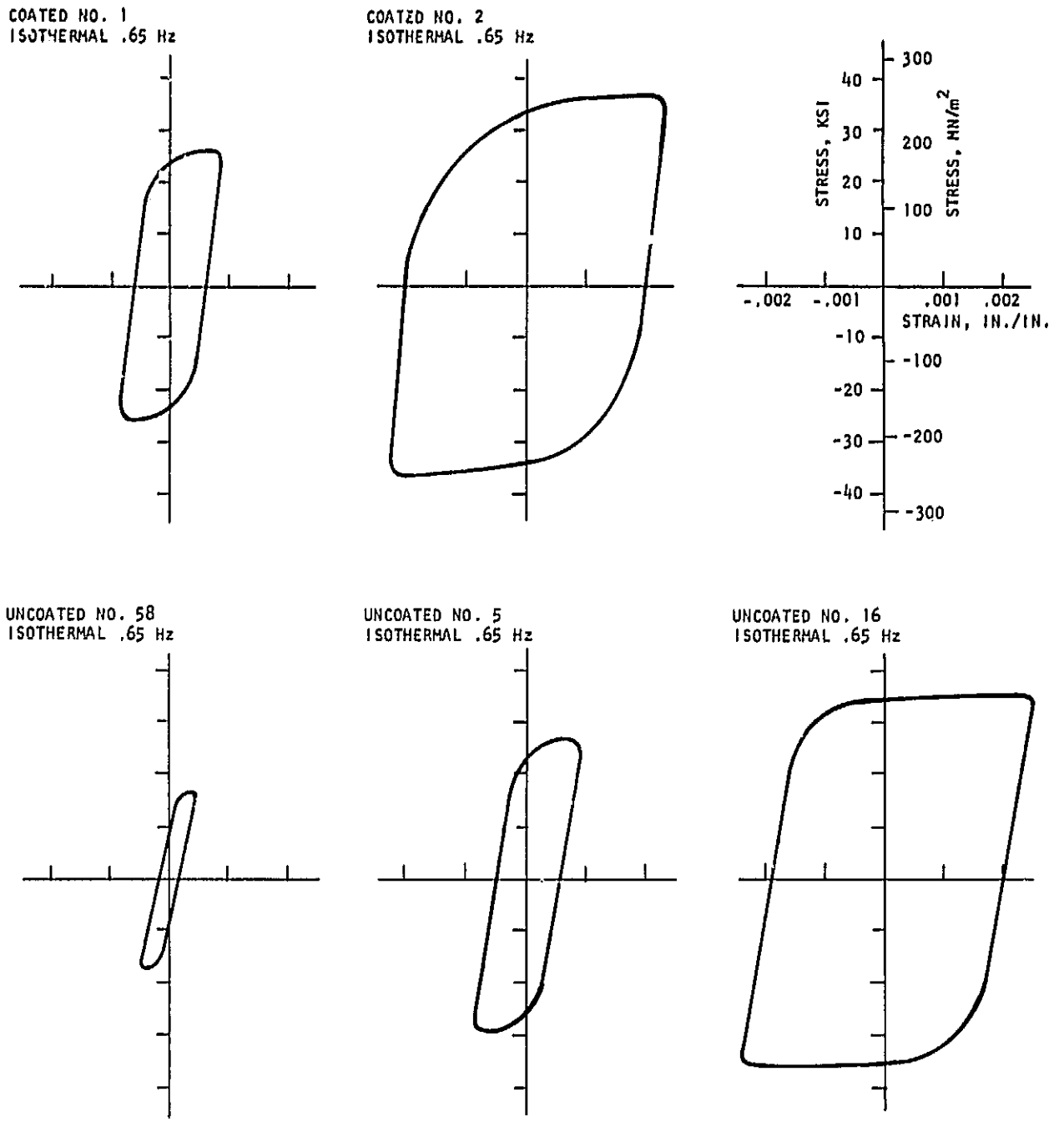

Figure B-1. Hysteresis Loops for Isothermal Tests Performed at 1000°C (1832°F), 0.65 Hz.

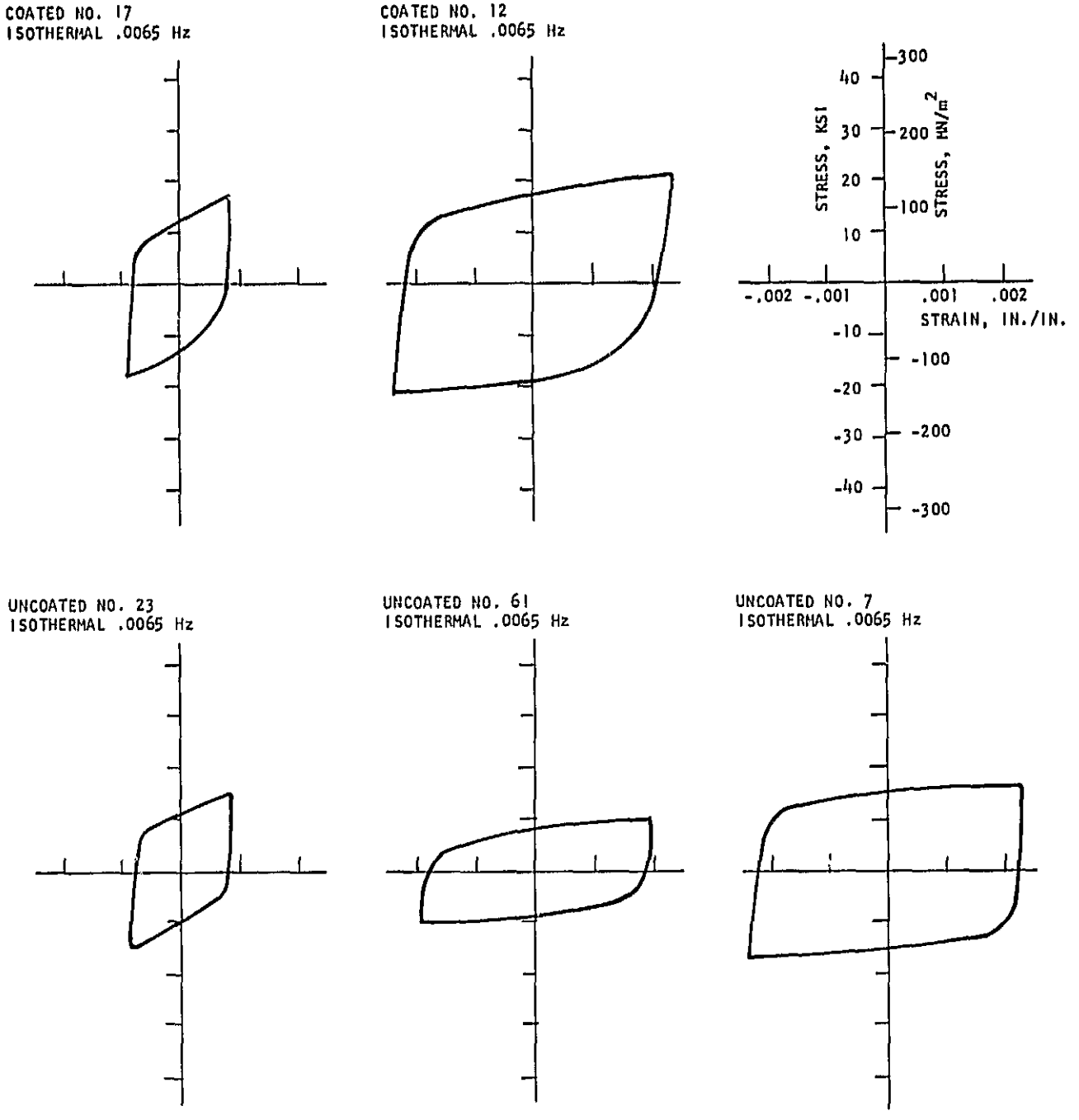

Figure B-2. Hysteresis Loops for Isothermal Tests Performed at 1000°C (1832°F), 0.0065 Hz.

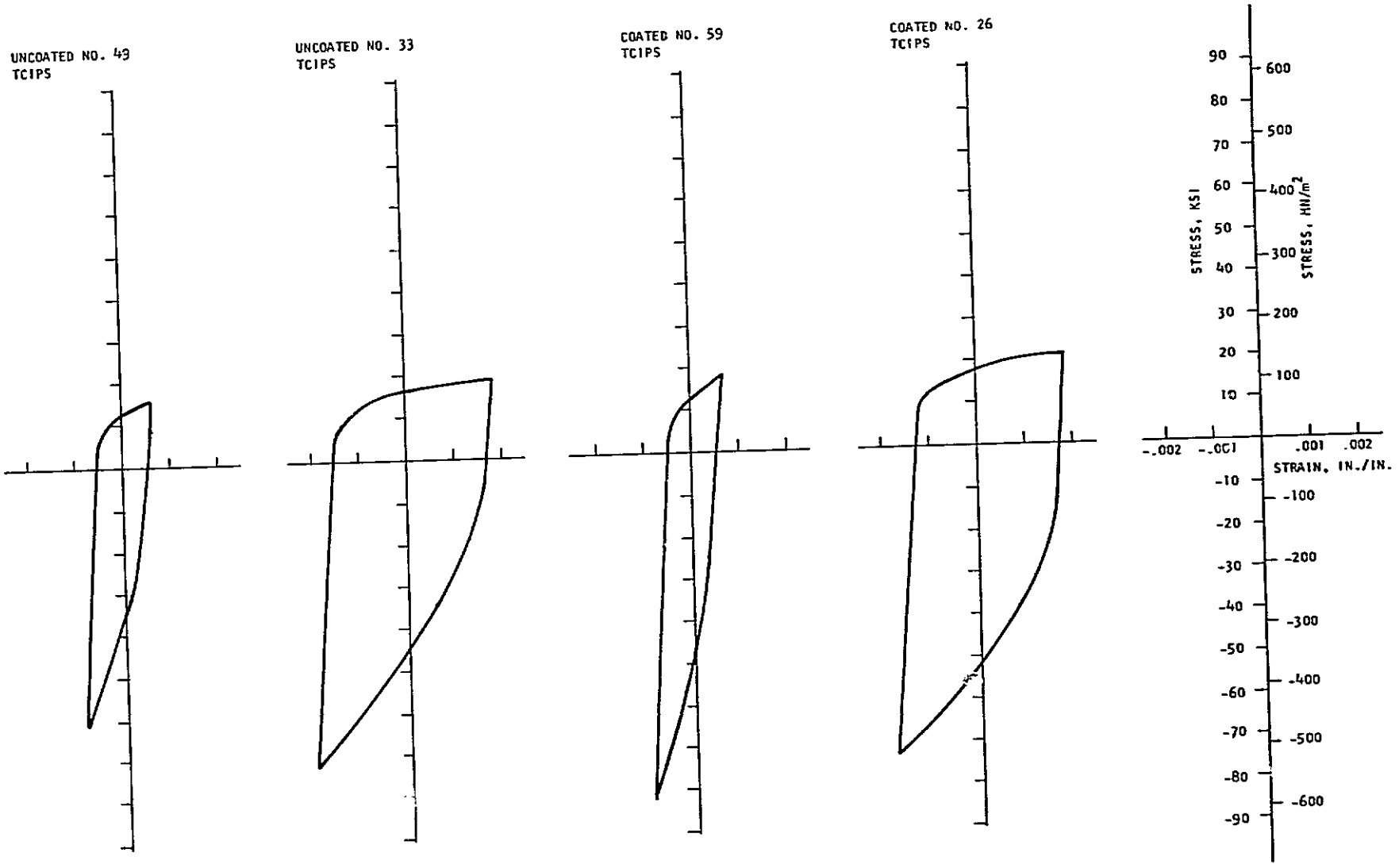

Figure B-3. Hysteresis Loops for TCIPS Tests.

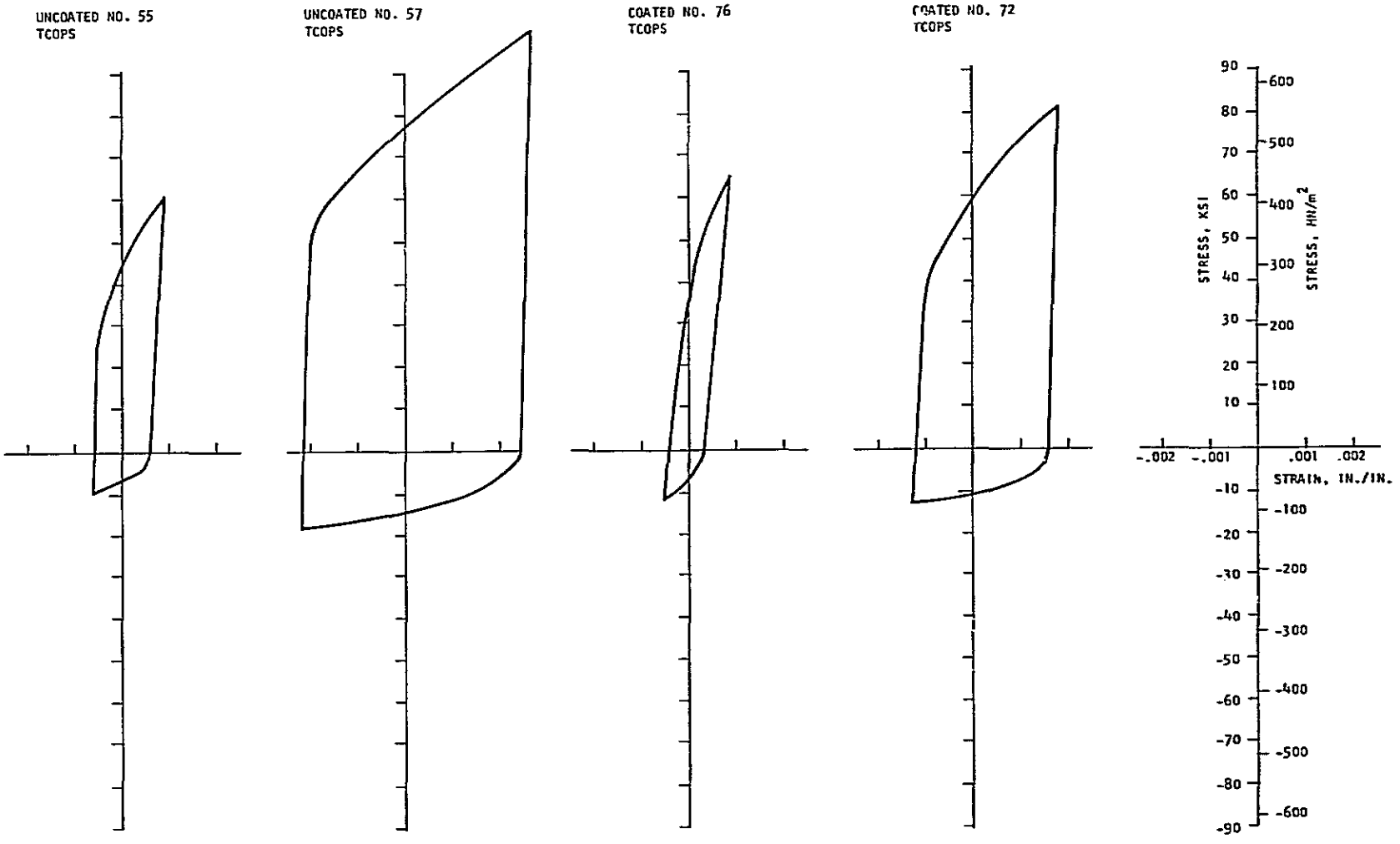

Figure B-4. Hysteresis Loops for TCOPS Tests.

APPENDIX C

STRESS VERSUS CYCLE CURVES

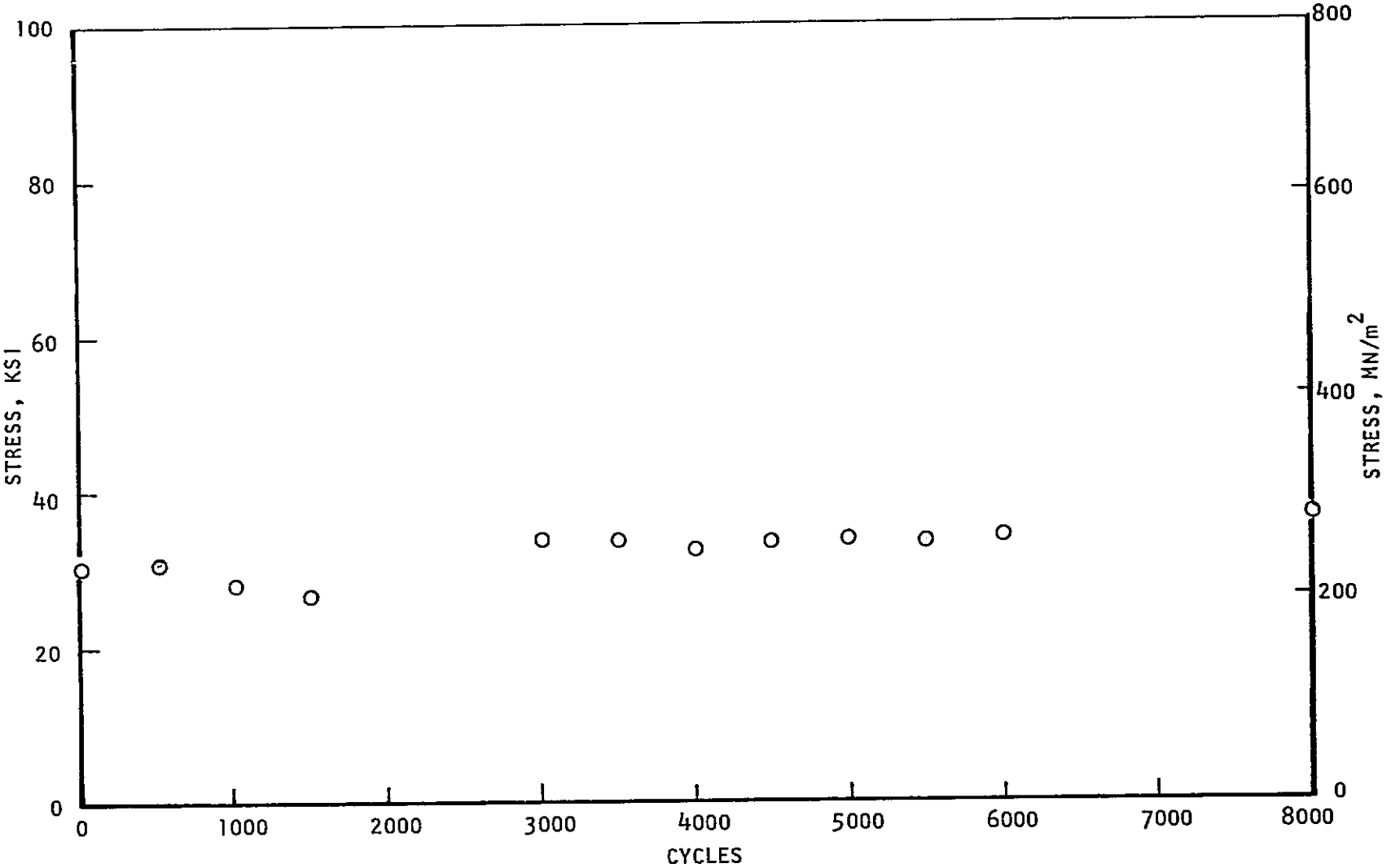

Figure C-1. Specimen No. 58 Uncoated Isothermal 0.65 Hz at 1000°C (1832°F) Total Longitudinal Strainrange .00301, Cycles to Failure 9433.

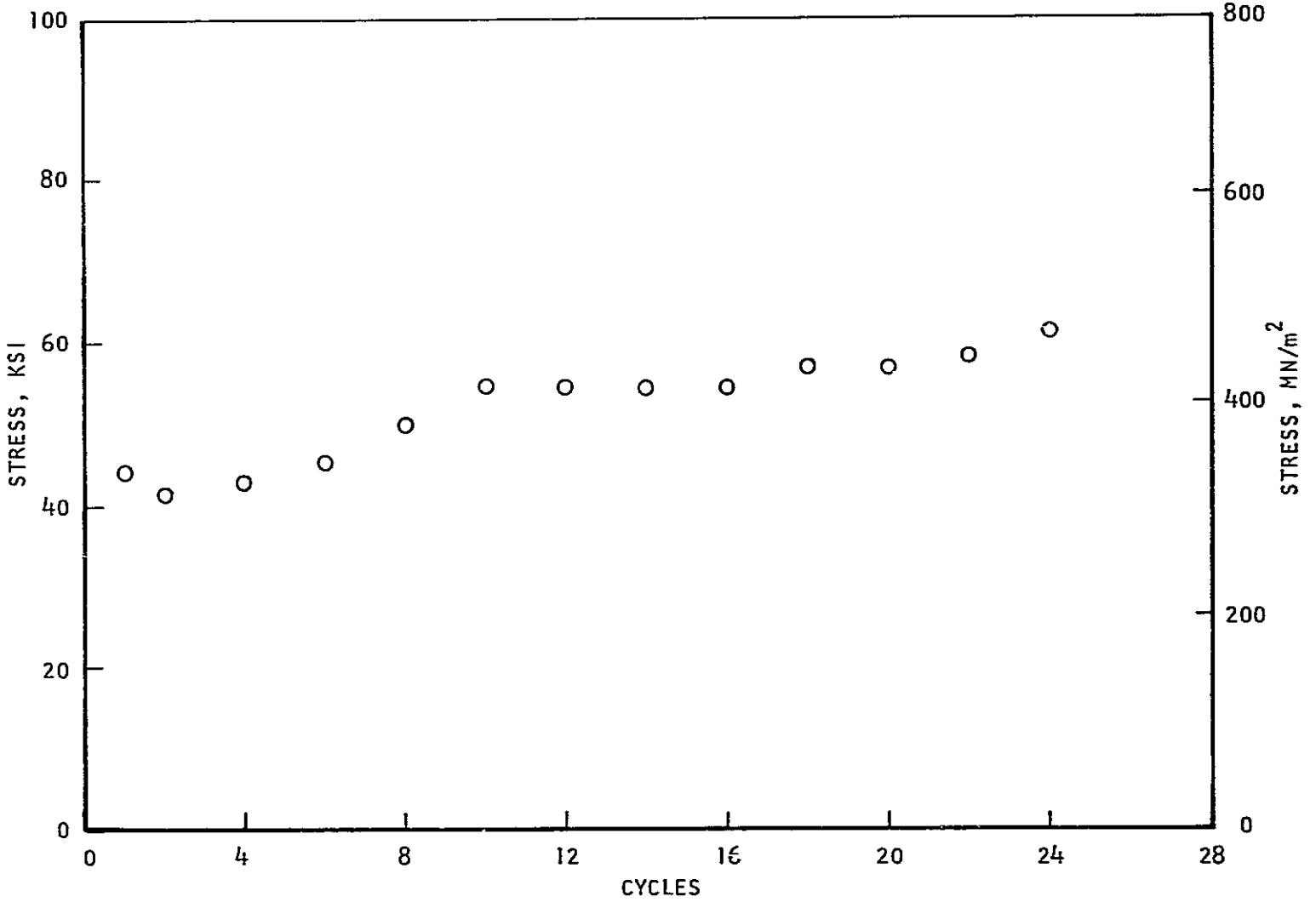

Figure C-2. Specimen No. 5 Uncoated Isothermal 0.65 Hz at 1000°C (1832°F) Total Longitudinal Strainrange .00671, Cycles to Failure 968.

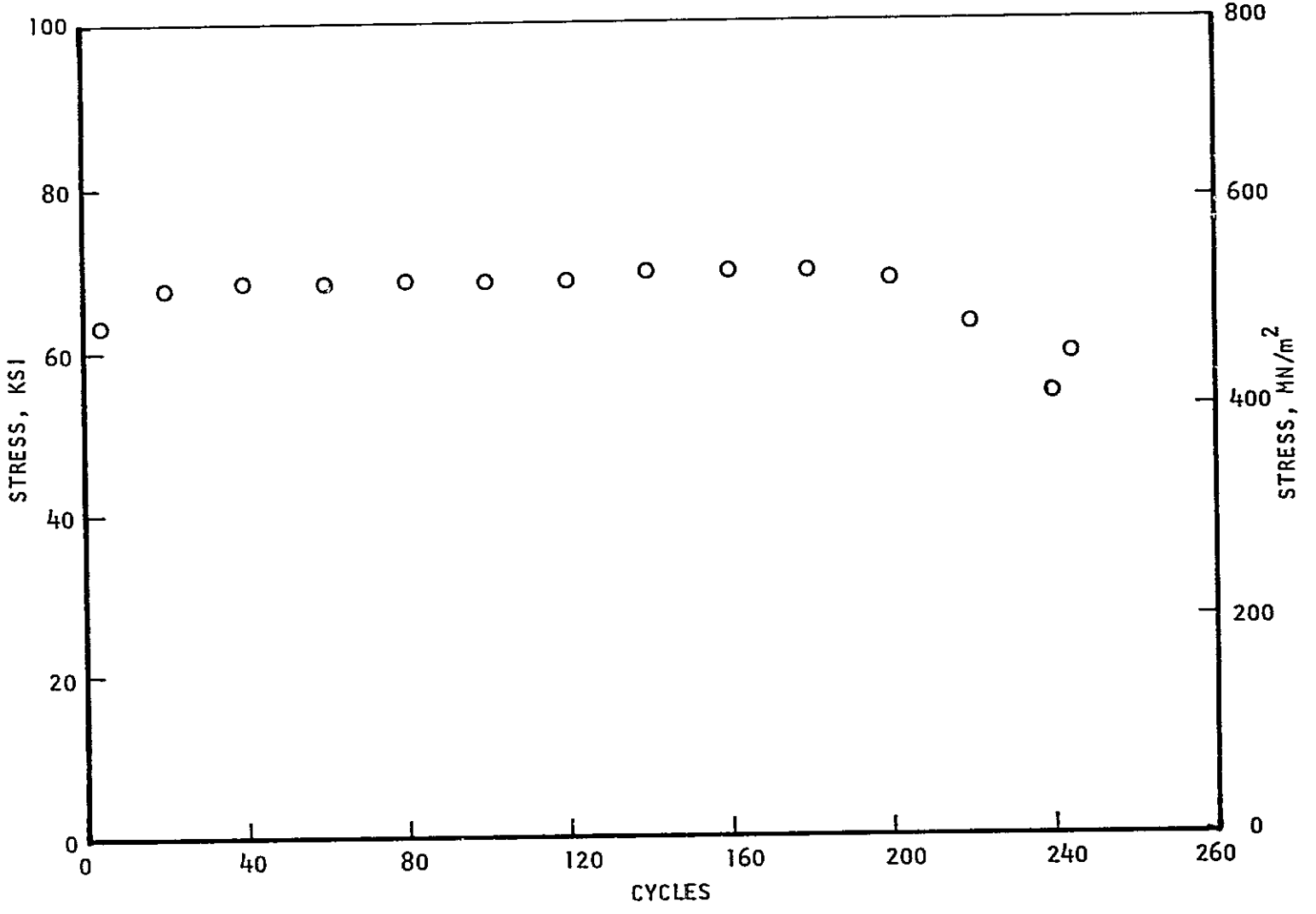

Figure C-3. Specimen No. 16 Uncoated Isothermal 0.65 Hz at 1000°C (1832°F) Total Longitudinal Strainrange .01388, Cycles to Failure 245.

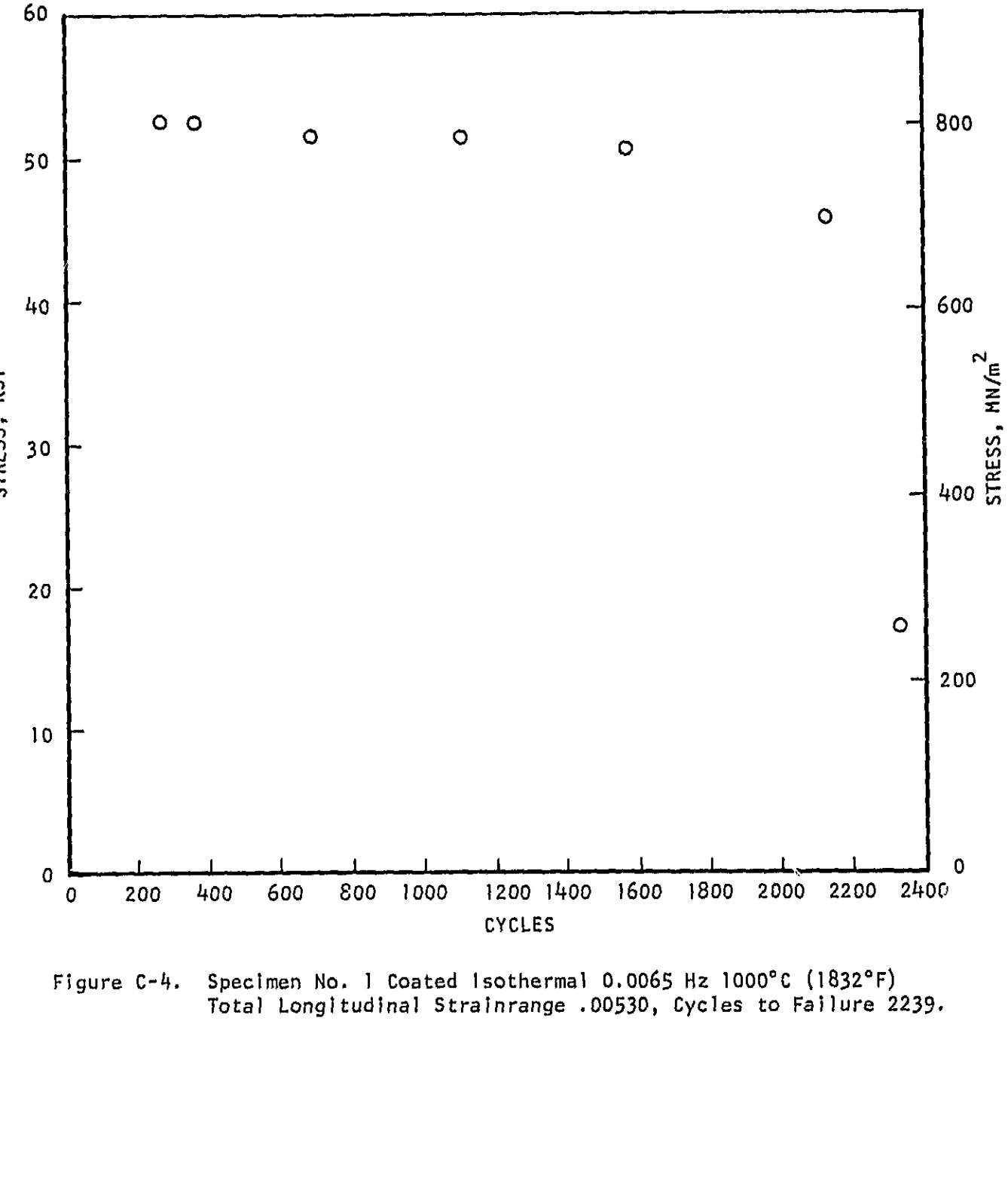

Figure C-4. Specimen No. 1 Coated Isothermal 0.0065 Hz 1000°C (1832°F) Total Longitudinal Strainrange .00530, Cycles to Failure 2239.

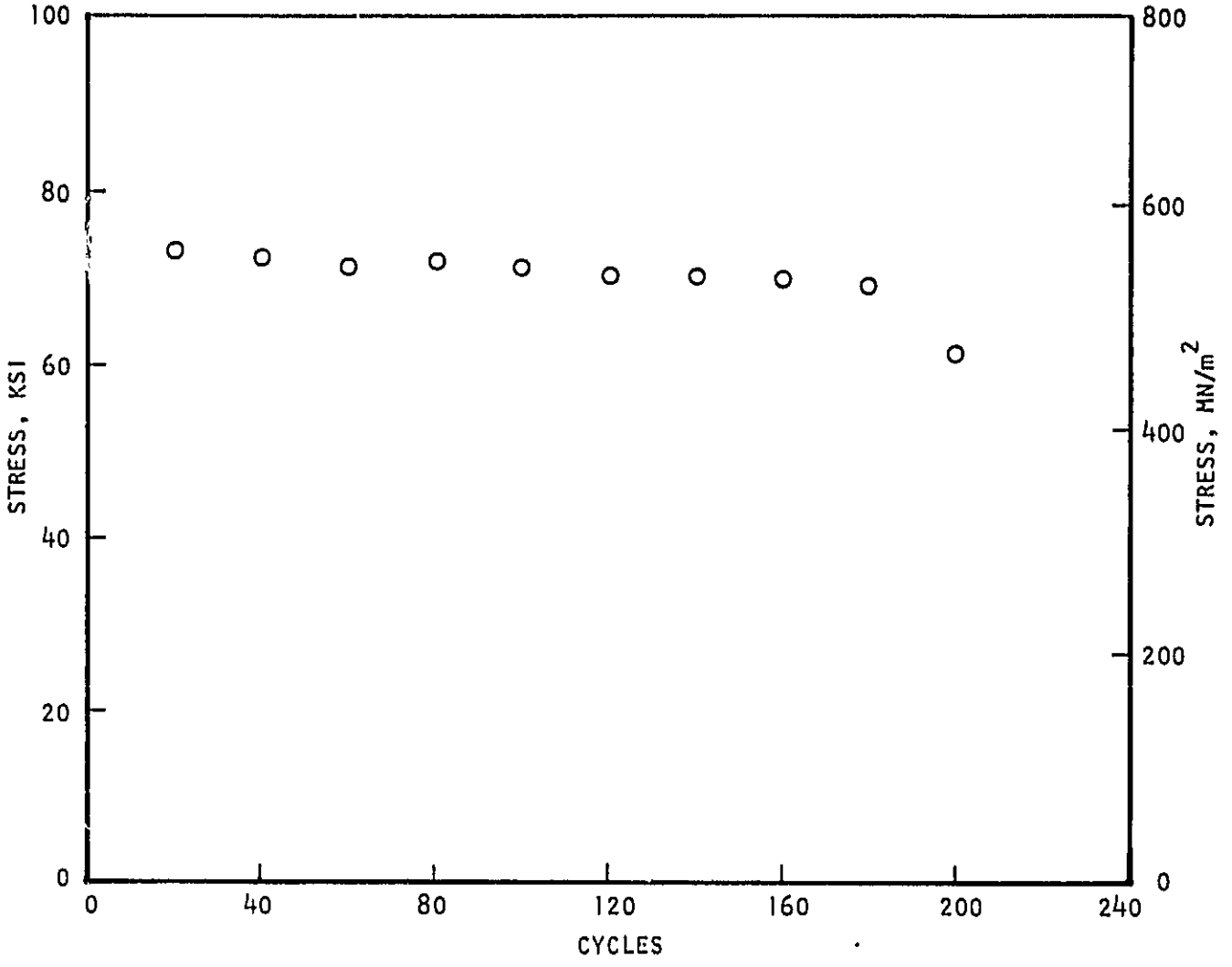

Figure C-5. Specimen No. 2 Coated Isothermal 0.0065 Hz 1000°C (1832°F) Total Longitudinal Strainrange .01160, Cycles to Failure 201.

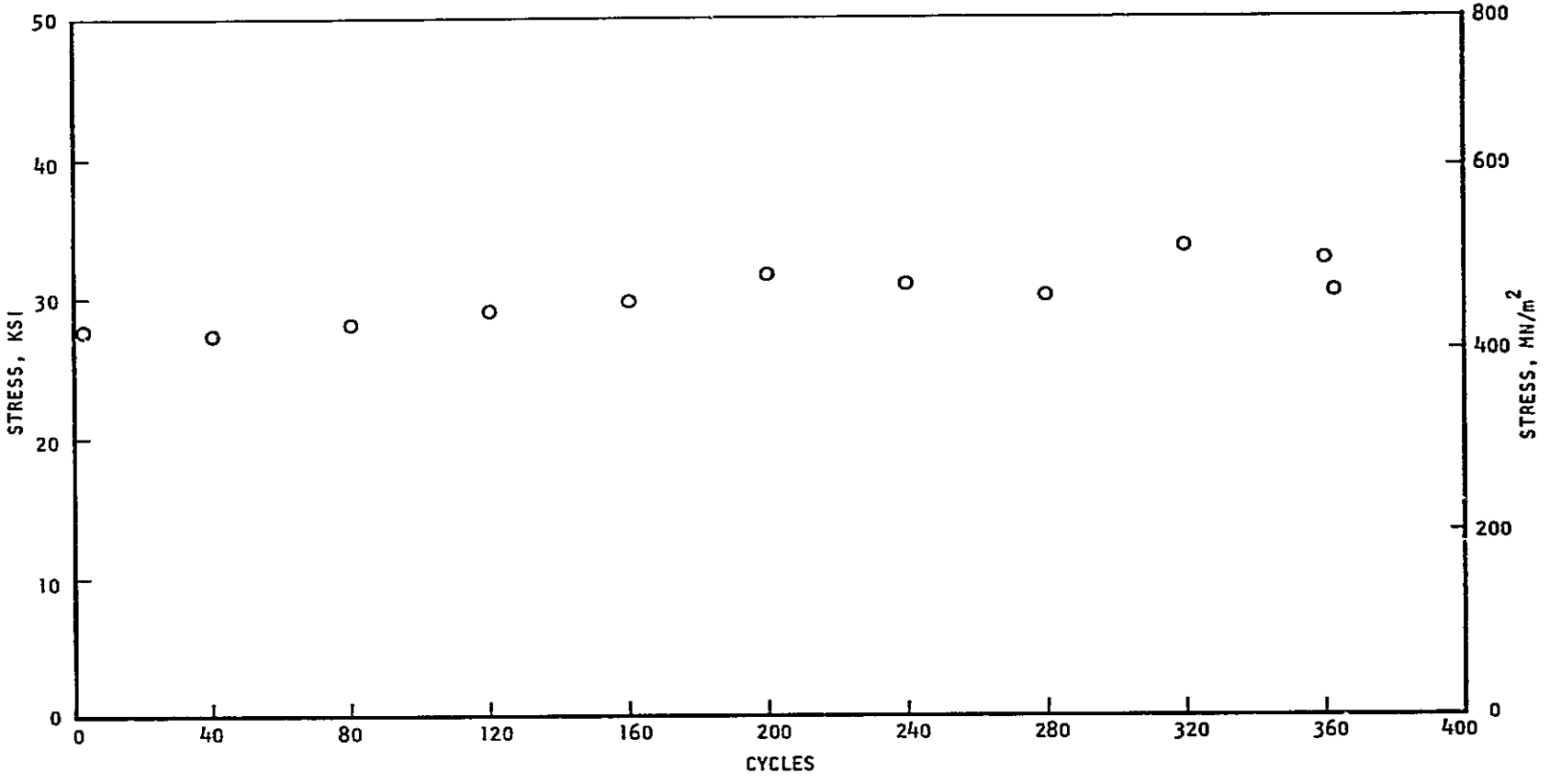

Figure C-6. Specimen No. 23 Uncoated Isothermal 0.0065 Hz 1000°C (1832°F) Total Longitudinal Strainrange .00424, Cycles to Failure 364.

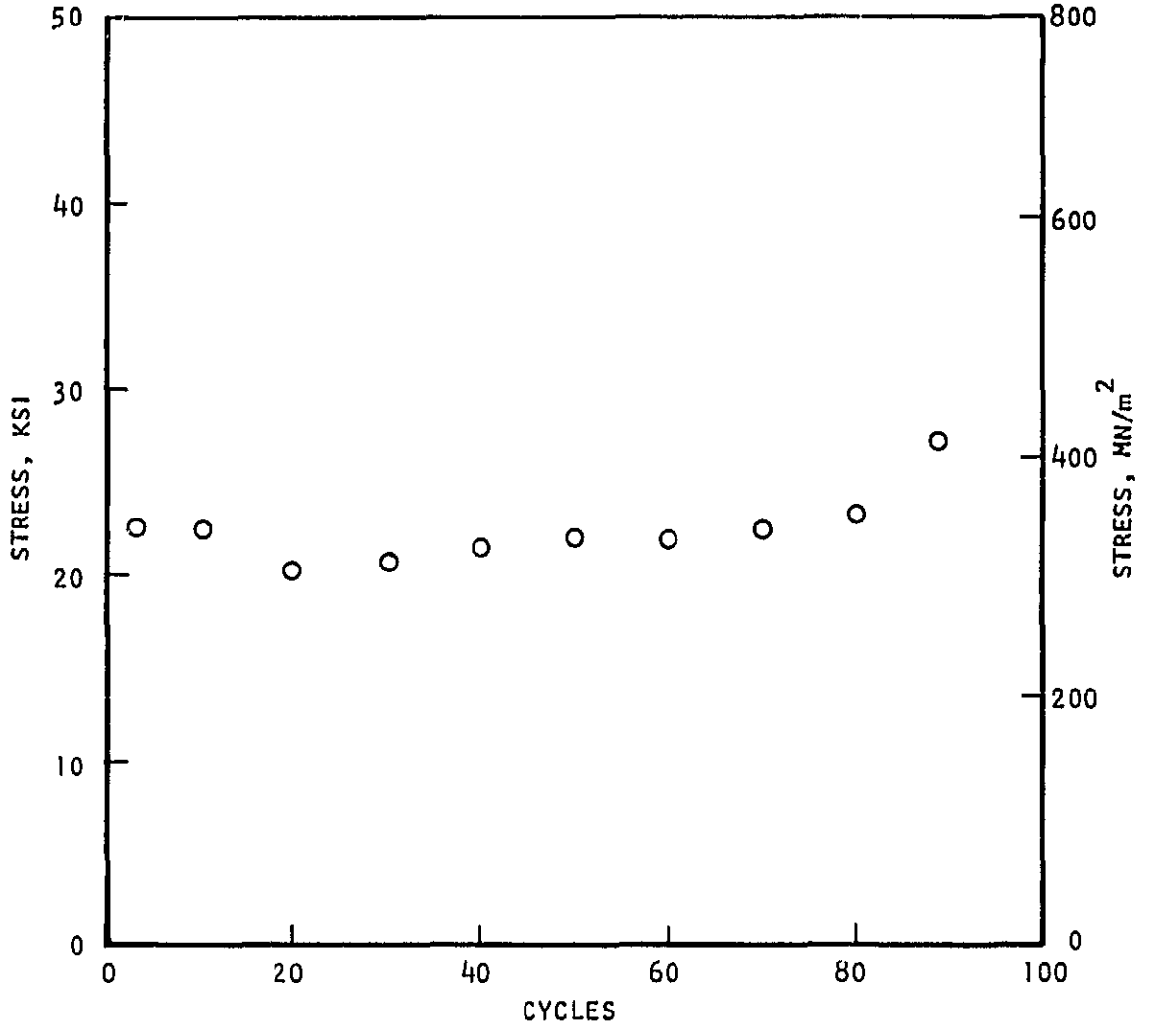

Figure C-7. Specimen No. 61 Uncoated Isothermal 0.0065 Hz 1000°C (1832°F) Total Longitudinal Strainrange .00881, Cycles to Failure 90.

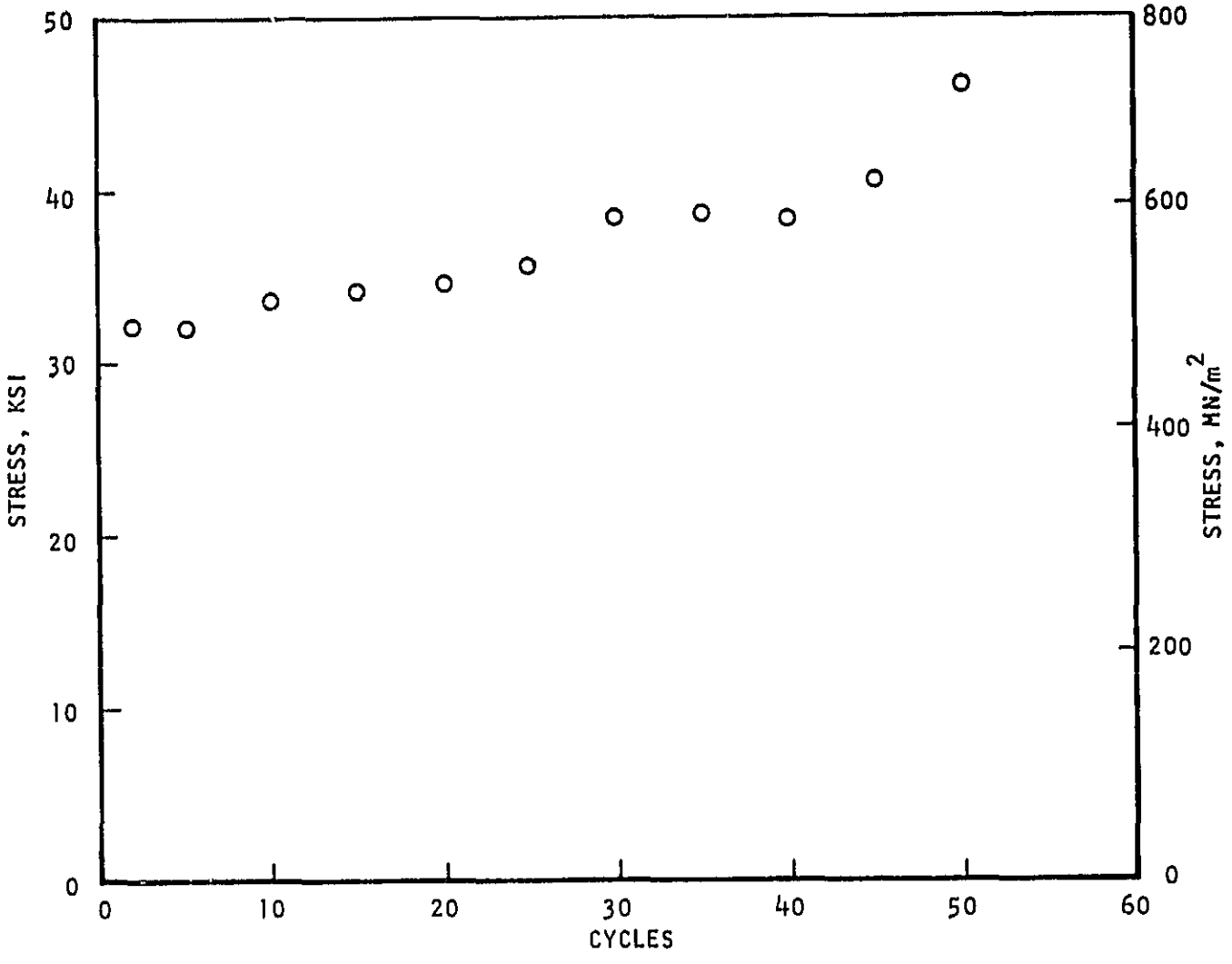

Figure C-8. Specimen No. 7 Uncoated Isothermal 0.0065 Hz 1000°C (1832°F) Total Longitudinal Strainrange .01090, Cycles to Failure 52.

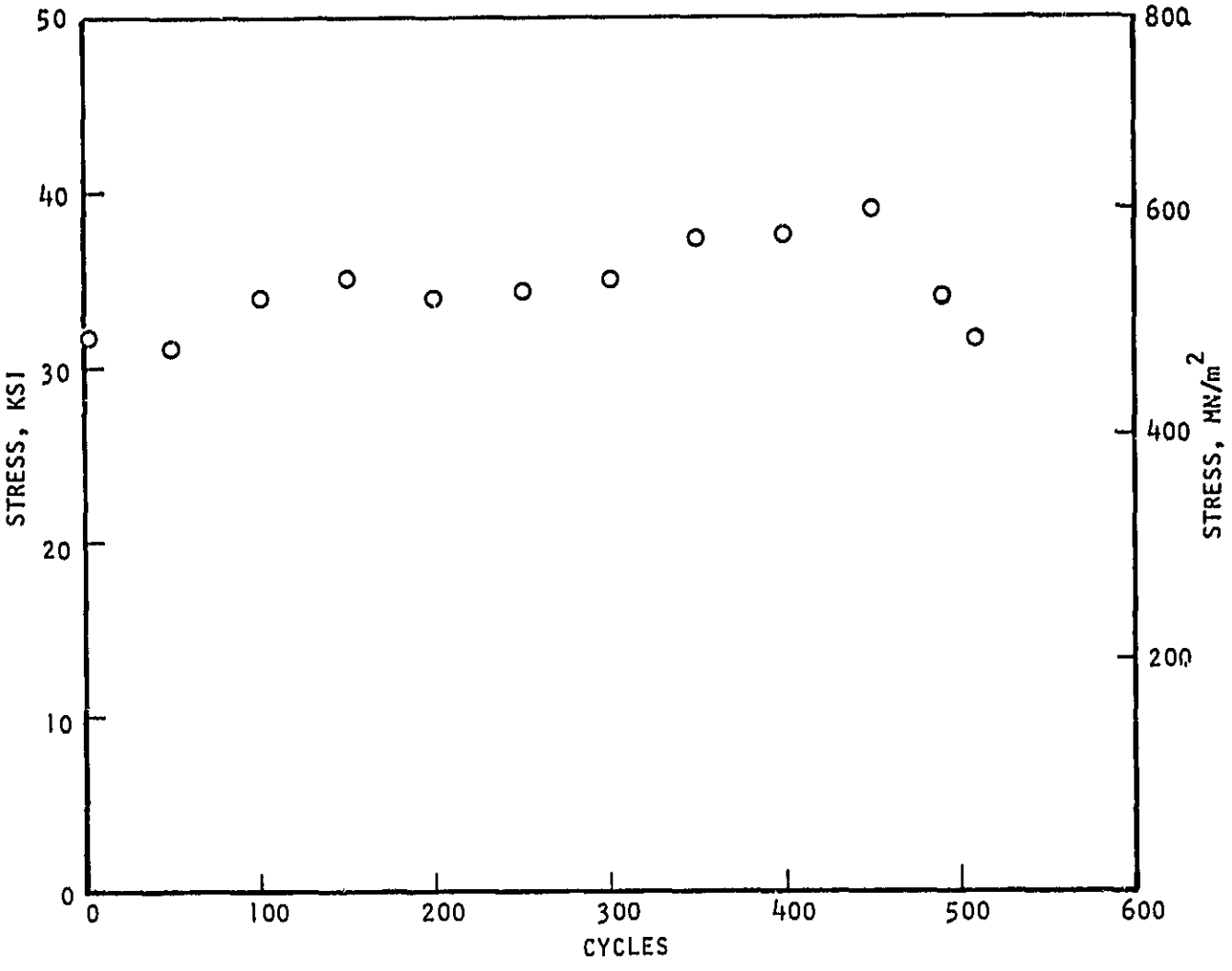

Figure C-9. Specimen No. 17 Coated Isothermal 0.0065 Hz 1000°C (1832°F) Total Longitudinal Strainrange .00427, Cycles to Failure 511.

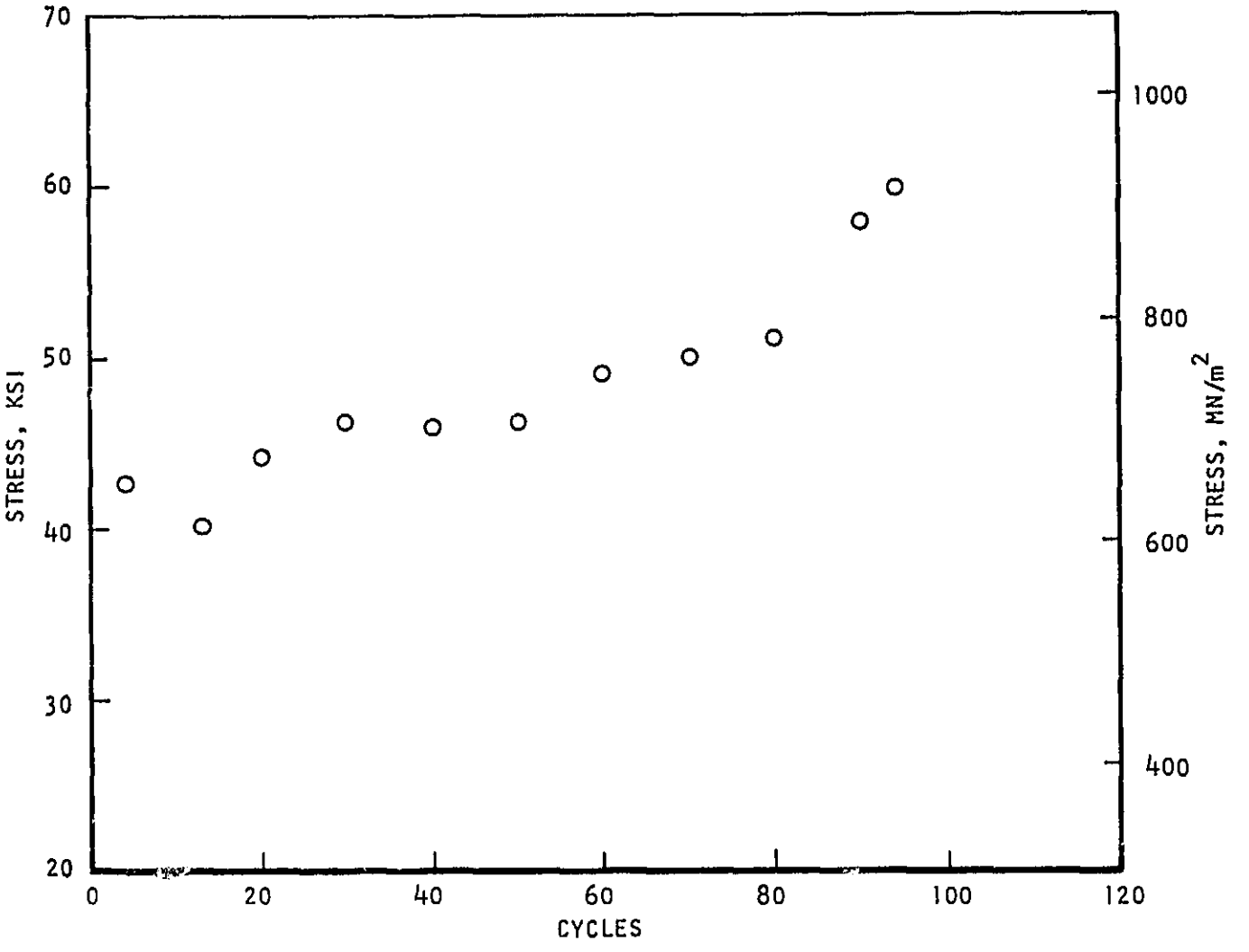

Figure C-10. Specimen No. 12 Coated Isothermal 0.0065 Hz 1000°C (1832°F) Total Longitudinal Strainrange 0.01005, Cycles to Failure 95.

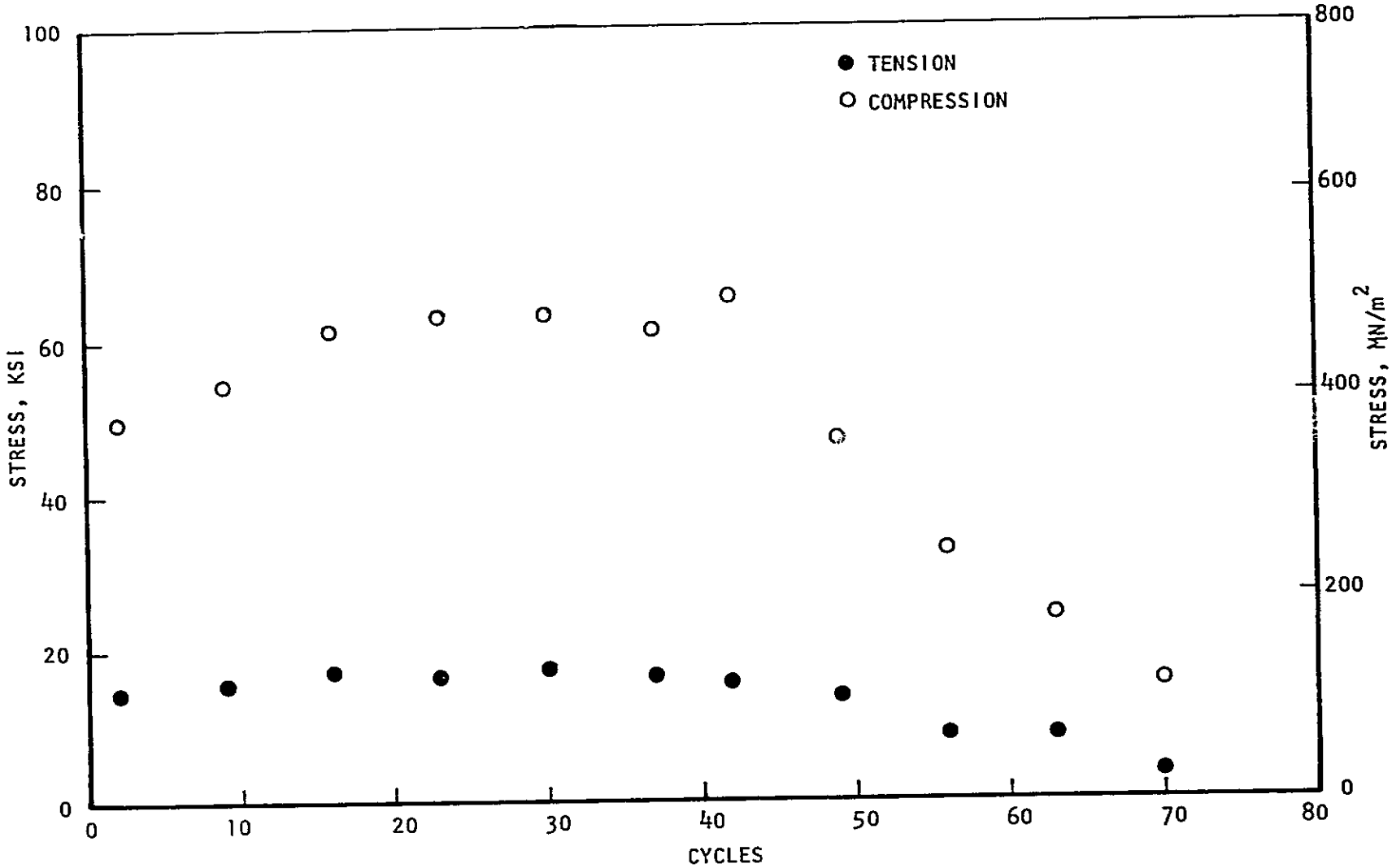

Figure C-11. Specimen No. 49 Uncoated TCIPS 0.0065 Hz 1000/500°C (1832/932°F) Total Longitudinal Strainrange 0.00408, Cycles to Failure 71.

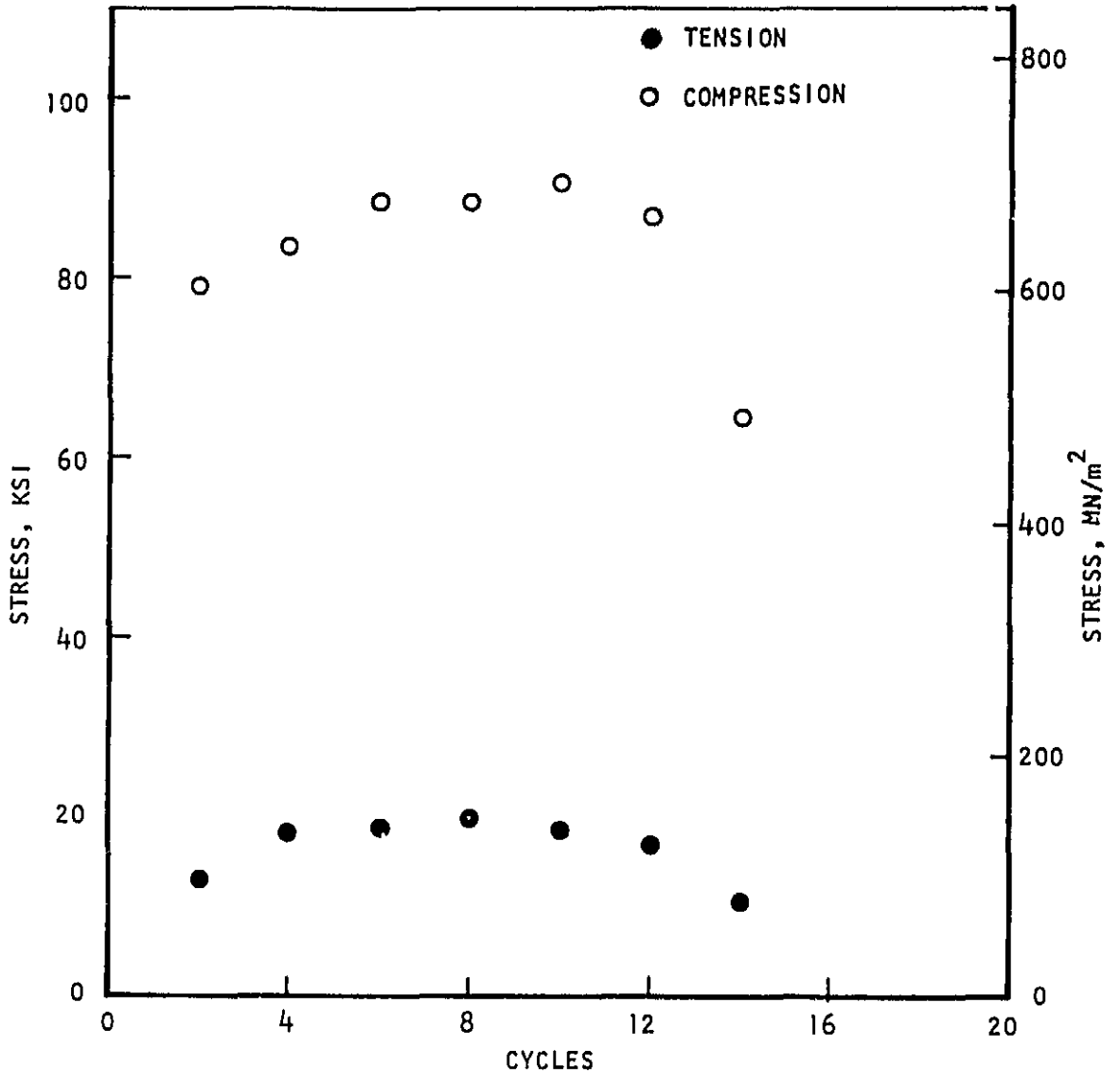

Figure C-12. Specimen No. 33 Uncoated TCIPS 0.0065 Hz 1000/500°C (1832/932°F) Total Longitudinal Strainrange .00895, Cycles to Failure 14.

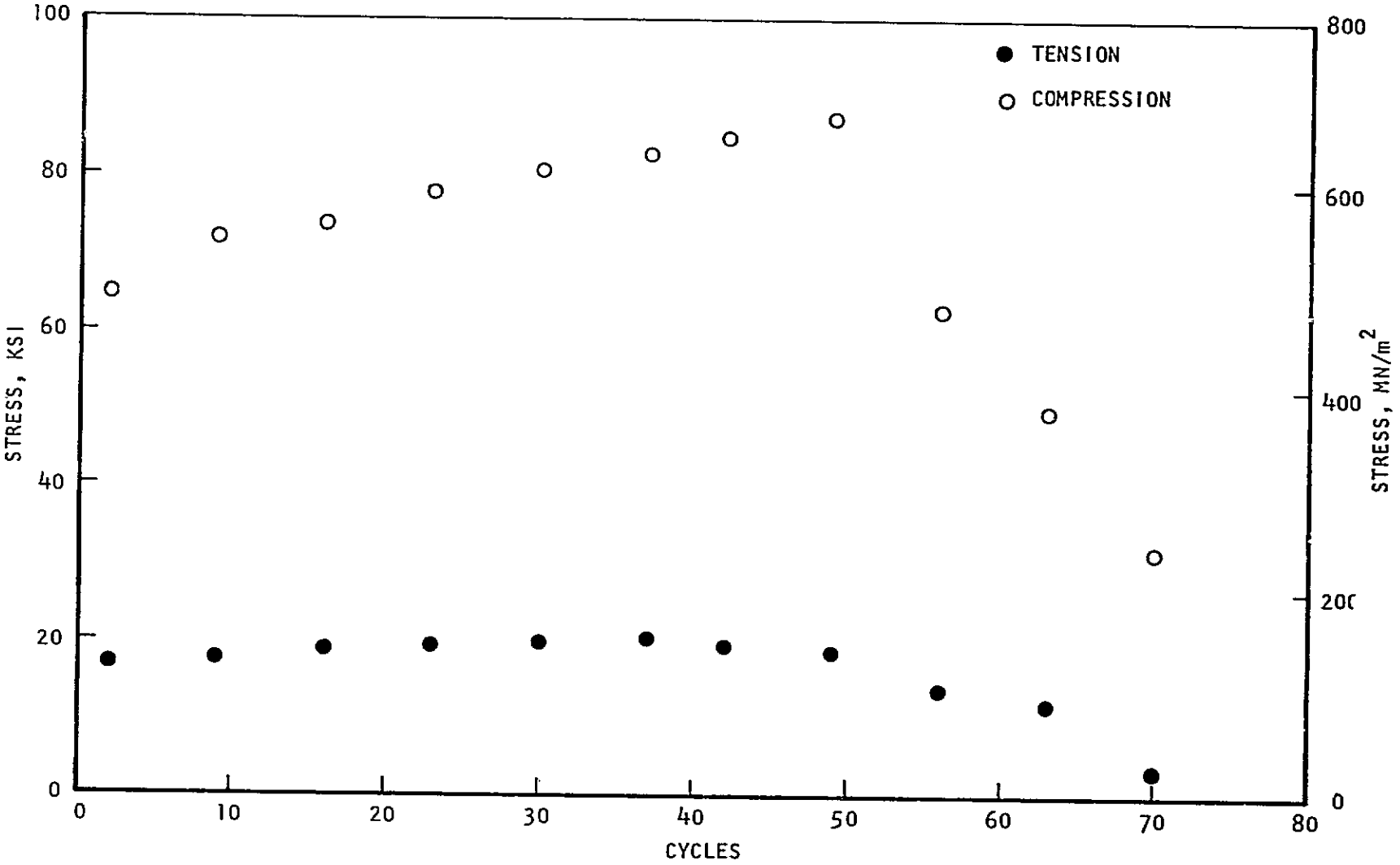

Figure C-13. Specimen No. 59 Coated TCIPS 0.0065 Hz 1000/500°C (1832/932°F) Total Longitudinal Strainrange .00444, Cycles to Failure 72.

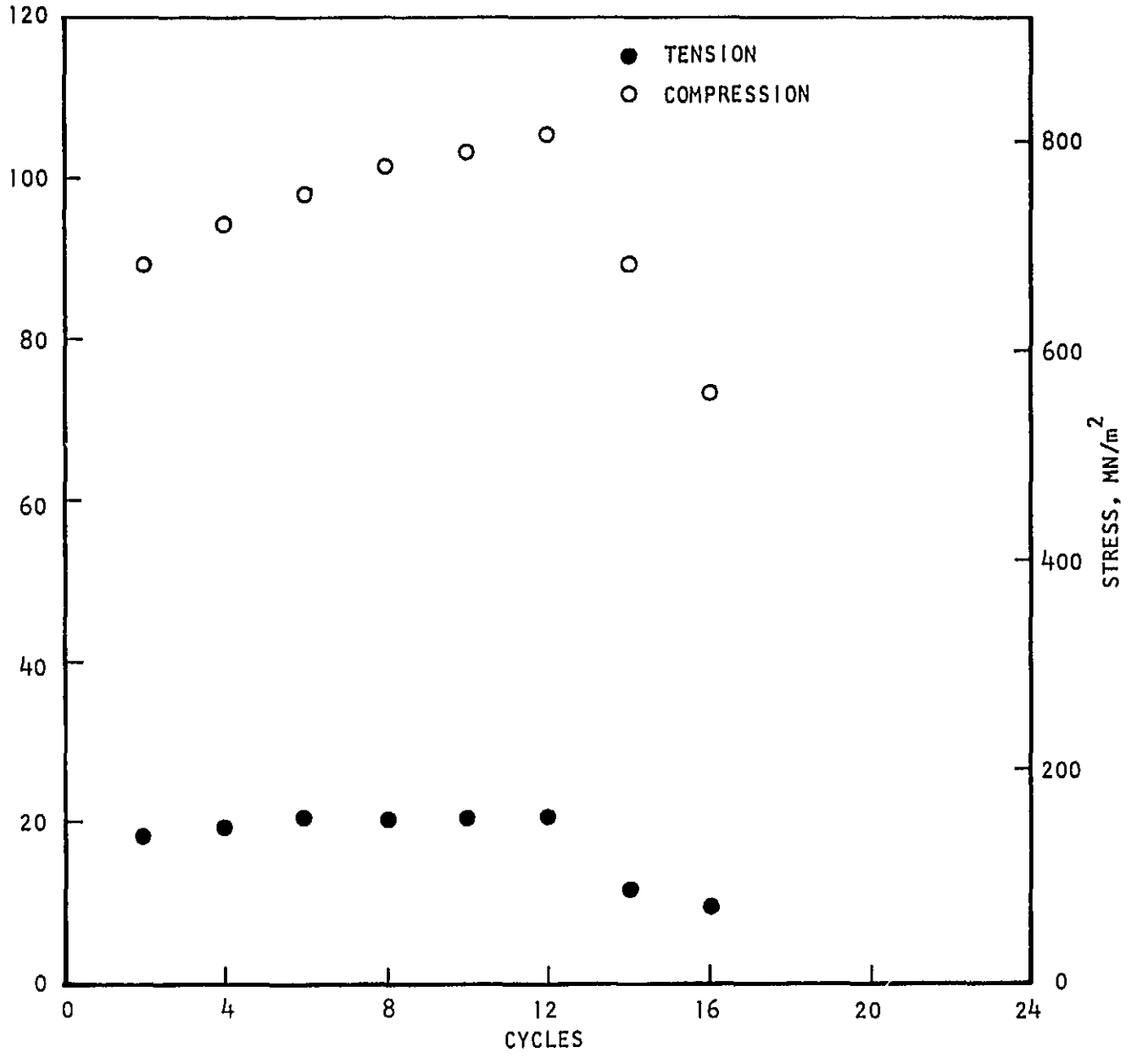

Figure C-14. Specimen No. 26 Coated TCIPS 0.0065 Hz 1000/500°C (1832/932°F) Total Longitudinal Strainrange .00861, Cycles to Failure 16.

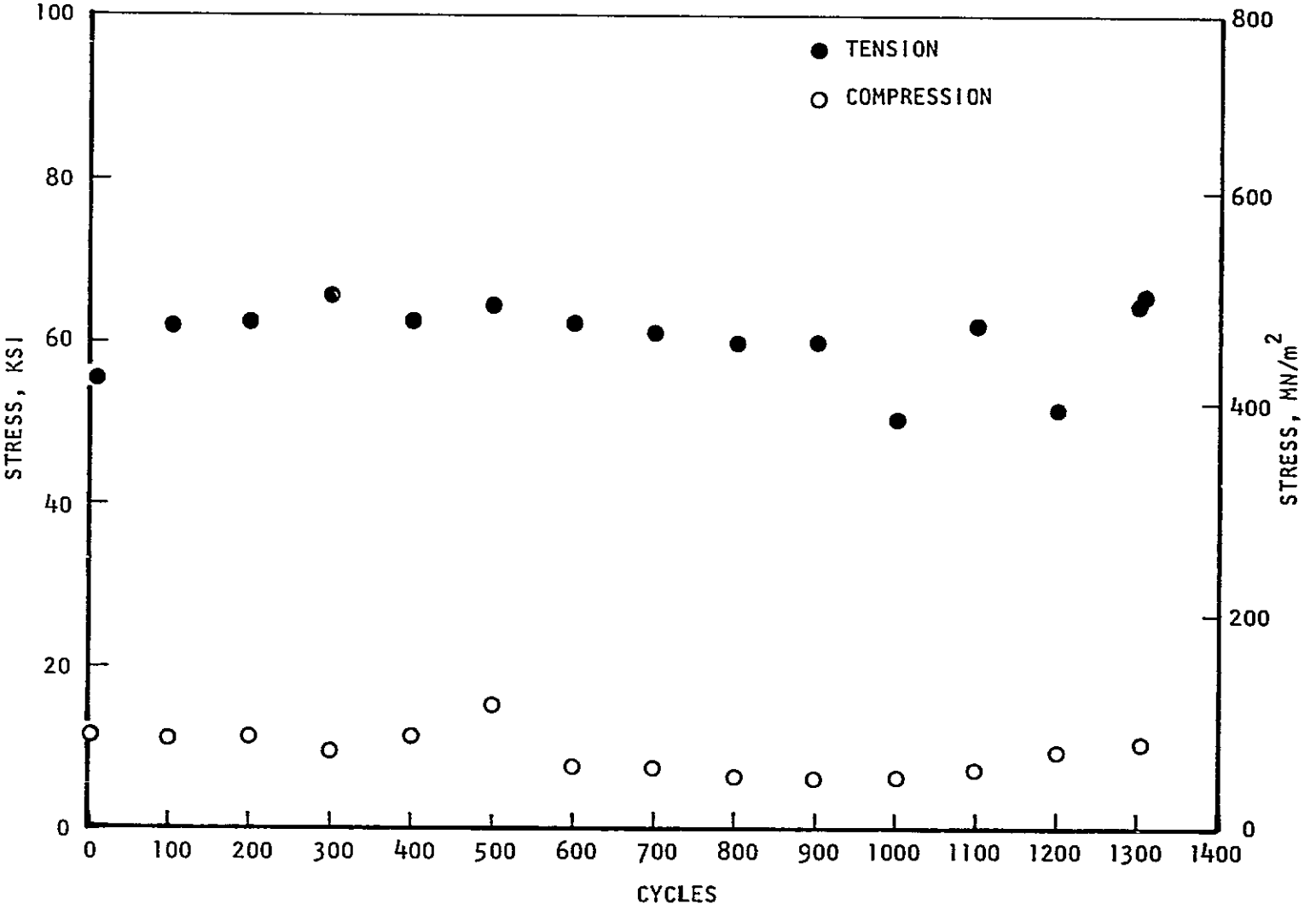

Figure C-15. Specimen No. 55 Uncoated TCOPS 0.0065 Hz 500/1000°C (932/1832°F) Total Longitudinal Strainrange .00405, Cycles to Failure 1308.

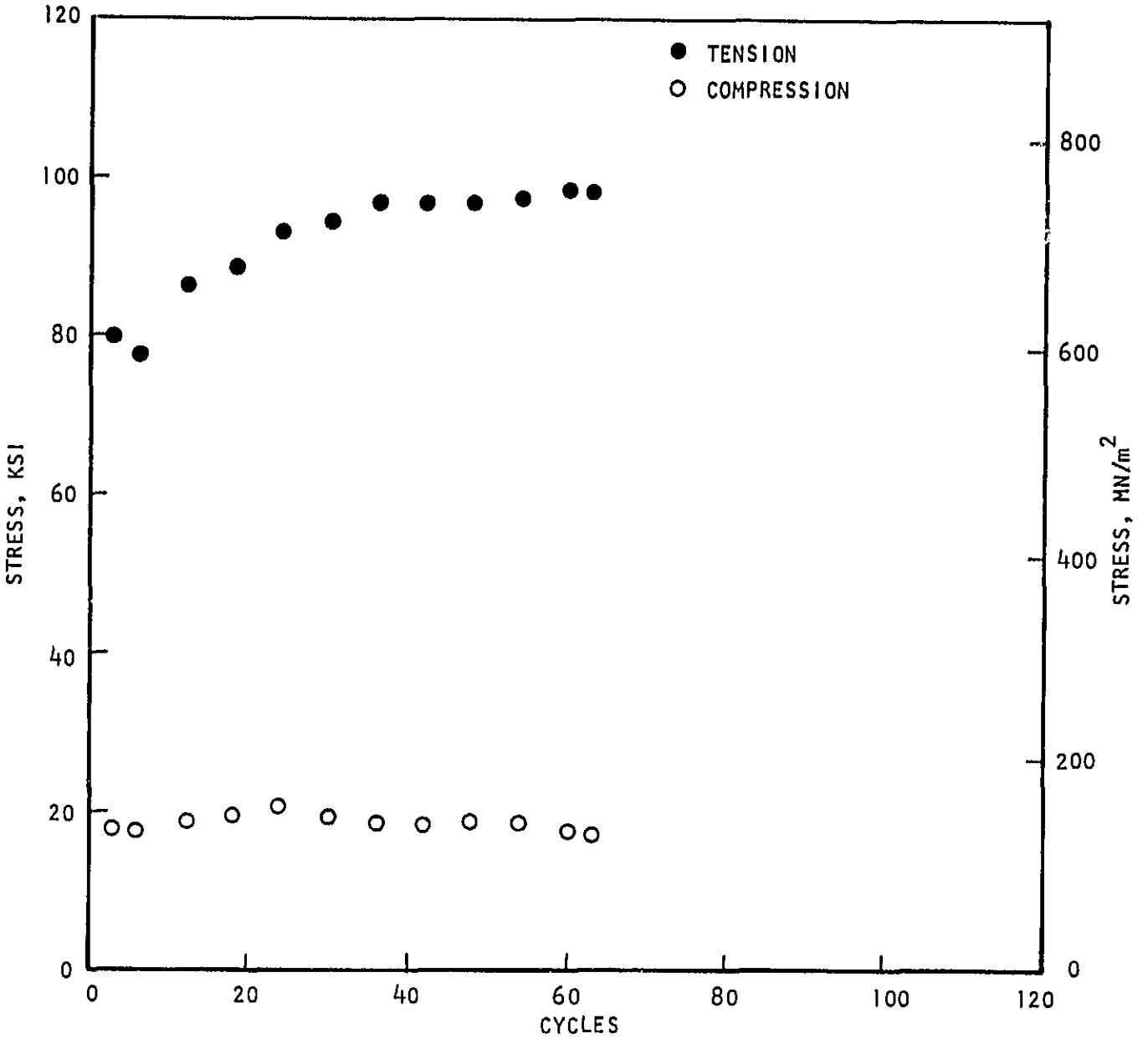

Figure C-16. Specimen No. 57 Uncoated TCOPS 0.0065 Hz 500/1000°C (932/1832°F) Total Longitudinal Strainrange .01126, Cycles to Failure 64. (Note: Specimen Failed Outside Gage Section)

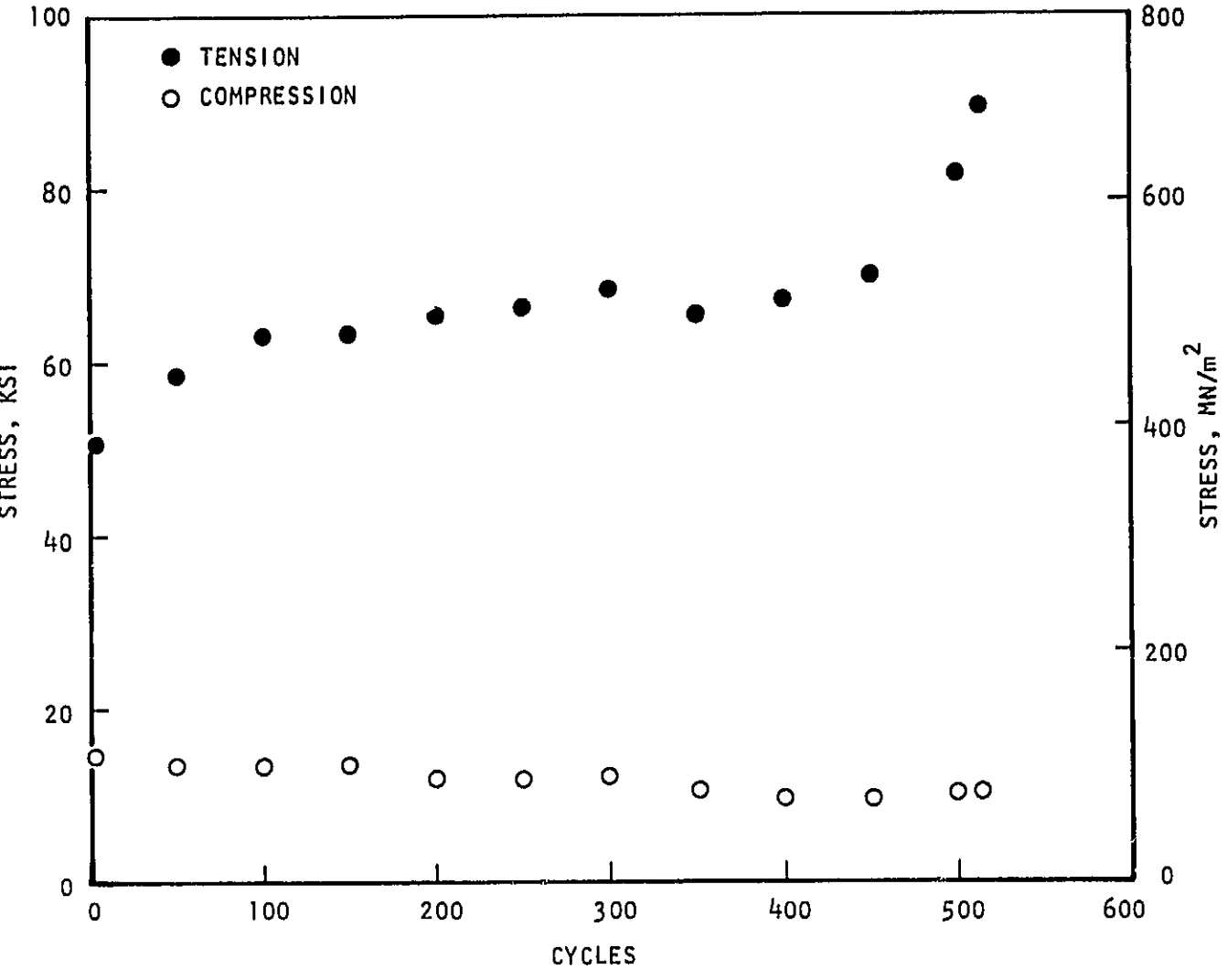

Figure C-17. Specimen No. 76 Uncoated TCOPS 0.0065 Hz 500/1000°F (932/1832°F) Total Longitudinal Strainrange .00410 Cycles to Failure 515. (Note: Specimen Failed Outside Gage Section)

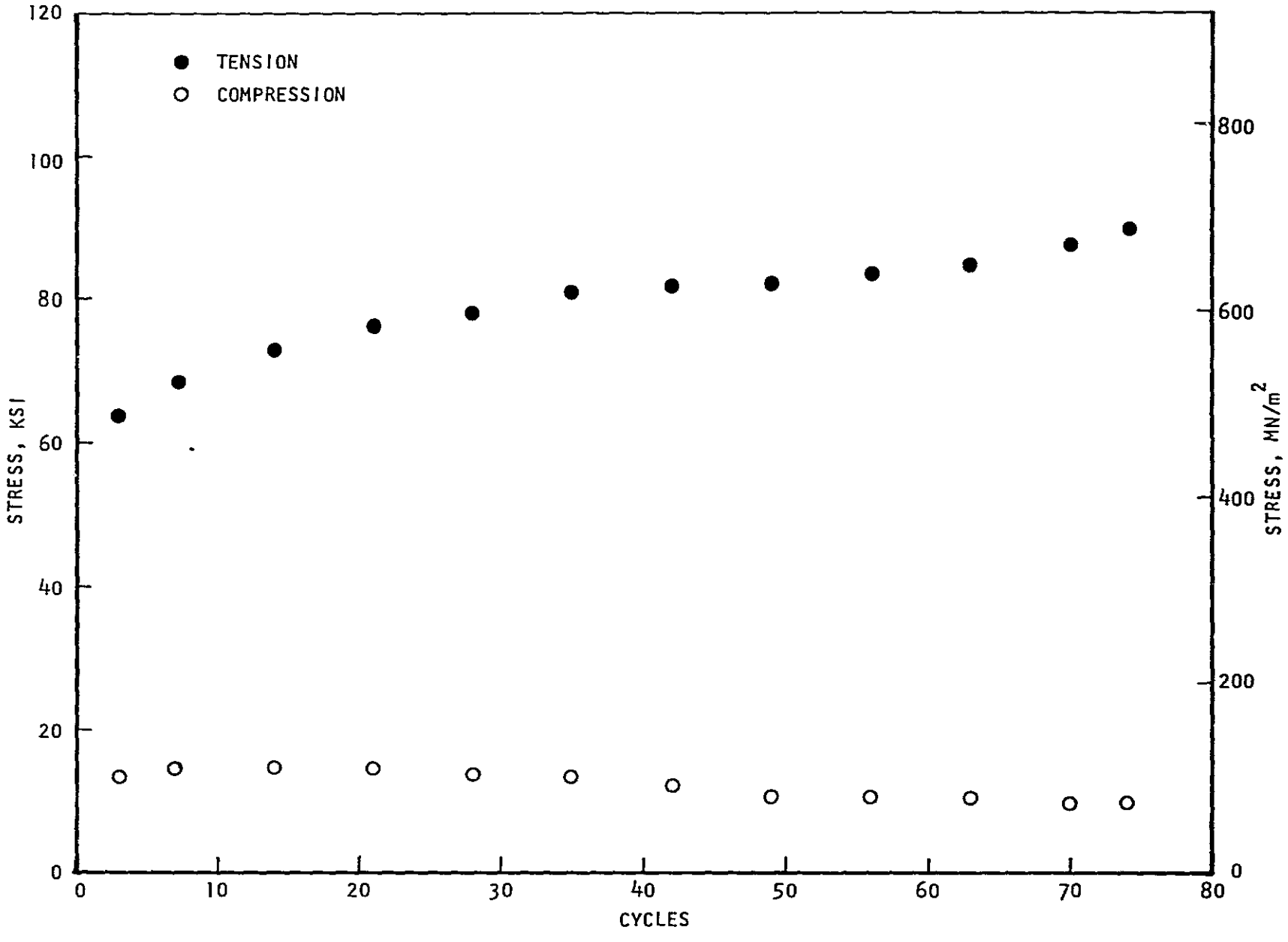

Figure C-18. Specimen No. 72 Coated TCOPS 0.0065 Hz 500/1000°F (932/1832°F) Total Longitudinal Strainrange .00939, Cycles to Failure 75. (Note: Specimen Failed Outside Gage Section)